Bioengineered *In Vitro* 3D Human Enteric Nervous System

A dissertation submitted by

Eleana Manousiouthakis

in partial fulfillment of the requirements for the degree of

Doctor of Philosophy

in

Biomedical Engineering

Tufts University

August 2019

copyright information if applicable: © 2019, Eleana Manousiouthakis

Adviser:

David L. Kaplan

Committee Members:

Kyongbum Lee

Kara Gross Margolis

Madeleine Oudin

ABSTRACT

The Gut-Brain axis is lauded as an avenue to understand and remedy many neurological and gastrointestinal disorders, with a focus on the gut microbiome in the years following the NIH human microbiome project [1-4]. The field was sparked in the early 2000s by the discovery that germ free mice showed enhanced response to stress by way of the hypothalamic-pituitary-adrenal (HPA) reaction, and this response could be ameliorated using certain pathogen free species [5]. The gut-brain axis is thought to include the central nervous system (CNS), the autonomic nervous system (ANS), the HPA, and the enteric nervous system (ENS) [6]. The ENS is the first neural system that gut content communicates with and thus represents a large target for bacterial metabolites. These microbial communities have an intimate relationship with host tissue and have been implicated in mucosal immune activation, reference memory, and anxiety-like behavior in mouse models [6, 7].

Much of the research being performed with respect to the ENS and the gut-brain axis is in animal models/tissues or in *in vitro* systems that currently do not have microbial capabilities [8, 9]. Our group has previously developed a silk-based scaffold with the capability of housing oxygen sensitive pathogenic and commensal microbes [10-12]. The goal of this work was to develop a 3D human *in vitro* intestinal tissue model to emulate the intricate cell interactions of the human enteric nervous system and the epithelial layer utilizing the previously developed model in order to better understand complex human conditions and microbial interactions that cannot be studied *in vivo*.

Here we describe a 3D innervated tissue model of the human intestine consisting of human induced neural stem cells (hiNSCs) differentiated into relevant ENS neural cell types, enterocyte-like (Caco-2) and goblet-like (HT29-MTX) cells forming the intestinal epithelial layer, and intestinal myofibroblasts (IMF) as the stromal layer. *In vitro* enteric nervous system (ivENS) cultures supported survival and function of the various cell biomarkers (nNOS, TAC1, NK1, MUC2, Muc5AC, and TuJ1), with mucosal and neural transcription factors evident over 5 weeks. Next, ivENS were inoculated using microbial metabolites, taurine (T) and kynurenate (K), prior to treatment with lipopolysaccharides (LPS) from *E. coli*. Results from these various treatment conditions indicated that metabolites contribute a potential protective effect against the pro-inflammatory response of cytokine monocyte chemoattractant protein-1 (MCP-1) production. This innervated tissue system offers a new tool to use to help in understanding neural circuits controlling the human intestine and associated communication networks.

ACKNOWLEDGMENTS

David Kaplan, thank you for being an amazing mentor throughout this PhD. You have not only been supportive of all the work I have done within the lab, but you have been supportive of my career goals and outside science communication projects. Thank you for taking a chance on me and helping me develop as a researcher, collaborator and mentor. Your support for both myself and my students over the years means the world to me.

Kyongbum Lee, Madeleine Oudin and Kara Gross Margolis, thank you for gracing me with your intellect, advice, and support over the course of this work. You have all been a fantastic committee and I appreciate all you've done for me.

Nicholas Alden, you have been a joy to work with I could not have asked for a better collaborator. Not only are you an intelligent researcher, your organization and friendly attitude have allowed the research hiccups to remain mere hiccups.

Ying Chen and Dana Cairns, thank you for always being willing to help me out, whether it was weekend text messages, or going over methods and statistics for those triple and quadruple checks. You both have been so supportive of this work and I am so thankful to have had you both on my team.

Milva Ricci, no words can describe what you mean to myself, and everyone else in this department. Grazie mille. Gwen Buchanan, Laura Place, Keleigh Sanford, Kim Ellwood, Bruce Panilaitis, Laura Suarez, and Rosa Mazzeo thank you for helping to keep this department, this school, these buildings, and this lab running. Carmen Preda, you have guided us all through this lab and I am forever thankful for your support in making sure we are all doing ok, whether it was helping to fix broken pipettes or stopping for a friendly chat you help make this lab feel like home.

Maria Rodriguez, Meghan McGill, Nicole Raia, Sarah Bradner, and Sarah Lightfoot Vidal, thank you all for being the most fantastic cohort. I'm so happy we were able to share the last couple years together and support each other throughout this experience. I can't wait to see what you all do next. To my amazing undergraduates, Michael Dente, Olivia Hofheinz, Kaia Gerlovin, and Yasmin Razavi, your tenacity has been infectious. I have been so lucky to see you all develop as researchers especially in the face of failed assays and null data. I'm not sure who was doing the teaching in these arrangements, but I'm lucky to have had you all on Team ivENS. To the den of positivity crew, office 124c, Maggie Wang, Zaira Martin Moldes, Nina Dinjaski, William Cantley, Aswin Sundarakrishnan, Benjamin Partlow, Sophia Szymkowiak, Disha Sood, Craig Hanna, Andrew J. Stout, Natalie Rubio, John Yuen, Maria Rodriguez, Maria Montero, and Katie Jordan, this PhD would not have been the same without you. Thank you for sharing your funny stories and troubleshooting ideas. It's been a wild ride and you all made it perfect. Jonathan Grasman, Siwei Zhao, Morgan Hawker, Whitney Stoppel, the four of you are such an inspiration, I am so happy we were able to keep our peer mentoring group running for so long. You have taught me what it means to be an academic and a mentor, thank you for all the early breakfast conversations and congratulations on your faculty positions we are 4/4. Terrence Roh, Yu-Ting Dingle, Olga Liaudanskaya, Rotimi Bolonduro, Jessica Stieglitz, Morgan Taylor, Josef Bober, Elena Jacobson, Miryam Adelfio, Mattia Bonzanni, Rachael Parker, Andrew Ford, Vincent Fitzpatrick, James Lin, Philip Houtz, Nick Fiore, Nic Rouleau, Josh Erndt-Marino, Queeny Dasgupta, Tyler Marcet, Onur Hasturk, Manisha Raghavan, Kyle Fish, Wenda Zhou, Harry Paul, Michael Lovett, Thomas Nieland, Holden Friend, Craig Mizzoni, Will Collins, thanks for having my back in the lab and my need to chit-chat. Thank you to every single person in the Kaplan Lab, Oudin Lab, Lee Lab, Georgakoudi Lab, Van Deventer Lab, in SciTech, and the SEC. You all made this project possible and we shared so many lovely moments together.

Zach Glass, Matteo Stoppato, Nate Schiele, Laura Hockaday, and Kaori Graybeal, I would not have gotten into or through this program without you all. Thank you for believing in me even when I was struggling and thank you for everything that you taught me.

The Manousiouthakis Crew: Mom, Dad, Irene, and Yanni. Thank you for pushing me to move across the country and for always believing in me. I’m so happy to know that I have all your love and support.

Paddy, this dissertation has been such a crazy experience, thank you for sharing it with me. Thank you for proofreading my writing, bringing me food to the lab on all those late nights, hanging out with me even when “it’ll only be like 30 minutes” turned into 2 hours, and being a solid support system. You have been so generous with your time and have always supported my pursuit of this research.

TABLE OF CONTENTS

LIST OF TABLES

LIST OF FIGURES

ABBREVIATIONS

ANS = Autonomic Nervous System

CNS = Central Nervous System

ENS = Enteric Nervous System

GI = Gastrointestinal Tract

hiNSCs = Human Induced Neural Stem Cells

HN = Human Nuclear Stain

HPA = hypothalamic-pituitary-adrenal

IMF = Intestinal Myofibroblasts

KO = Knockout

NGF = Neural growth factor

SP = Substance P

CHAPTER 1 : INTRODUCTION

The overall goal of this research was to develop, characterize, and optimize an ex-vivo tissue model of the enteric nervous system, with focus on the epithelial and neuronal interactions. This chapter provides the background information on the biology of the endogenous enteric nervous system, current animal and bioengineered models used to study the enteric nervous system, and an overview of the aims of this research. Components of this section have been adapted from [13]

BACKGROUND

The Gut-Brain axis has presented an interesting avenue to understand, and potentially remedy, many neurological and gastrointestinal (GI) disorders, particularly the microbiome-gut-brain axis [1-3]. The field was sparked in the early 2000s upon the discovery that the hypothalamic-pituitary-adrenal (HPA) reaction to stress was enhanced in germ free mice and that measures could be taken to partially correct this enhanced response to stress using specific pathogen-free species [5]. The bidirectional communication network of the gut-brain axis is thought to include the central nervous system (CNS), the autonomic nervous system (ANS), the HPA, and the enteric nervous system (ENS) [6]. The ENS is more affectionately called the "brain in the gut" and represents a large target for bacterial metabolites. These microbial communities have been implicated in mucosal immune activation, reference memory, and anxiety-like behavior in mouse models [6].

The intestine is central to human health, and the ENS within the intestine functions as the main component of the autonomic nervous system. The number of neurons within the ENS rivals that of the neurons found within the spinal cord [14]. The ENS contains approximately 500 million neurons and quadruple that number of glia distributed throughout the intestine [15]. Although the ENS plays a central role in autonomy, functional control, and impact in the human body, bidirectional interactions between the CNS and the gastrointestinal tract (GI) via the enteric nervous system remain unmapped. This may be due in part to a lack of tissue models that focus on the epithelial and ENS interactions within the GI tract. Current intestinal systems for studying the enteric nervous system include murine or embryonic chick *in vivo* models, 2D cell culture, and organoids for transwell monolayers, and 3D *in vitro* models, with little focus on combining adult cell interactions, human derived cell sources, and microbiome crosstalk [8, 9, 16]. As such, improved ENS tissue models and understanding of such a system would have major implications in improving human health.

Research tools to help elucidate the role of intestinal neuromodulation in human health are essential. Current options are primarily limited to animal studies, cell culture studies, organoids, and related systems, all of which have inherent limitations (Table 1-1). The 3D microenvironment provides utility as well as geometric tunability for cellular cultures, mimicking physiorelavent conditions [10]. *In vitro* tissue engineered systems offer the potential to encompass the properties of endogenous human systems in a modular, tunable format.

Table 1-1: Current enteric nervous system landscape

System	Advantages	Limitations	Cell Source	Culture Time	Citation
Enteric Nervous System Organoids	1. Elucidate developmental processes and molecular mechanisms 2. Accessible to genetic manipulation 3. Can be made into monolayers	1. More closely mimics fetal intestine; immaturity of cells 2. Represent more of a regenerative state than a homeostatic state of the intestine 3. Lack of microbiome 4. Variability among organoids 5. Necrosis	Human, Mouse	4 weeks in vitro, 6-10 weeks post in vivo kidney capsule	[8, 9, 17]
In vivo systems	1. Complexity 2. Immune response 3. Microbiome 4. Accessible to genetic manipulation	1. Differences in the development of human and animal systems (ex. crypt development *in utero* in humans, but postnatally in mice; differences in tyrosine hydroxylase (TH^+) neuron development in mice and humans)	Mouse, Drosophila, Porcine	Long term, life of animal model	[8, 18, 19]
Innervated *in vitro scaffold*	1. Smooth muscle incorporated into system 2. Contractile tissue	1. Lack luminal surface 2. Lack of microbiome	Rabbit, Human	16 days, 14 days implanted in Rats	[20, 21]
Organ culture system	1. Maintains tissue architecture 2. Flow added to	1. Intestinal colonization proceeds progressively, model time scale is less than 2 days	Mouse	30-40 hours, ~24 hours with bacteria	[22]

	independently control the outside and inside of the lumen 3. Co-culture with the microbiome	2. Not suitable to long term responses to environmental perturbations			

The lack of a neuronal component in many intestinal models greatly limits the capabilities of *in vitro* systems to mimic the endogenous gastrointestinal environment. To address these limitations, we aimed to create a compartmental *in vitro* human intestine model to study neuromodulation at the gastrointestinal level while allowing for components to be adjusted or added as needed. Previously, we developed an expandable and rapidly differentiating human induced neural stem cell (hiNSC) line that allowed for spontaneous differentiation toward neural linage [23]. In addition, we have generated a 3D intestine model capable of months-long sustained access to these intestinal functions *in vitro* that ensures a reliable *ex vivo* tissue system for studies in a broad context of human intestinal diseases and treatments [10]. We hypothesized that if we innervated the model utilizing hiNSCs, we could use it to study the ENS, effectively creating an improved *in vitro* model that overcomes some of the drawbacks cited in **Table 1-1**. We developed *in vitro* 3D human innervated intestinal tissues with both human induced neural stem cells (hiNSCs) differentiated into pertinent enteric nervous system neural cell types, as well as enterocyte-like (Caco-2) and goblet-like (HT29-MTX) cells that create the intestinal epithelial layer, and intestinal myofibroblasts to support long term culture [10, 23]. This model elevates experimental options in technology to understand neural circuits controlling the intestine and can offer insight into those communicating with the microbiome. This system should be a welcome addition that combines the benefits of ***long-term culture and microbial interaction capabilities*** seen in *in vivo* systems, the ***human source material*** seen in organoid systems, and the ***compartmentalization and flexibility*** present in current *in vitro* systems.

SILK AS A BIOMATERIAL

Bombyx mori derived silk fibroin is a widely used natural polymer that has been lauded for its mechanical properties in addition to its biocompatibility and ease of modification [24]. Endogenous B. mori silk consists of two proteins, structural silk fibroin coated in sericin. For the purposes of most engineering applications the sericin protein is removed. The silk fibroin has a propensity to self-assemble into hydrophobic β-sheet structures, resulting in strong and resilient materials [24, 25].

Silk fibroin has the capability to be processed into sponges, tubes, hydrogels, splints, and films [26-30]. Silk has been utilized to recapitulate a variety of organs for various *in vitro* models, such as skin (6 weeks), cornea (4 weeks), and cortical brain tissue (3 weeks) [26, 29, 31, 32]. Silk systems have also shown their ability to sustain long term neurologically active *in vitro* cultures for 8 months, making this protein an ideal candidate for scaffold material [33].

The silk scaffold utilized in our work provides the structural integrity needed to replicate tissue architecture, containing a geometrically engineered hollow lumen to support studies of commensal or pathogenic cohorts that may have oxygen sensitivity found within the intestine. This is evident in previous work from our group that house parasitic *Cryptosporidium parvum* [11] and enteric bacterial pathogen *Yersinia pseudotuberculosis* [10]. *Y. pseudotuberculosis* experiments showcase low oxygen tension within the engineered lumen of our scaffold design by utilizing a hypoxia-responsive respiratory enzyme, fumarate reductase, to drive expression of the fluorescent protein genes, gfp, in hypoxic areas of the scaffold.

ENTERIC NEURAL DIVERSITY

The enteric nervous system (ENS) bares a close resemblance to the central nervous system, with neural components supported by enteric glia that abut their axonal bundles [34]. Within the two plexi of the ENS, neurons that mediate both motility and secretory activity of surrounding tissues are present, but it is still unknown at the transcriptional level precisely how enteric neural diversity is established [35]. The ENS can function independently from the CNS, but they typically communicate in a bidirectional manner [3]. To date, three major groups of neurons have been used to broadly categorize the myenteric plexus: motor neurons, intrinsic primary afferent neurons (IPANs), and interneurons (these ascend, descend, and/or project to the submucosal plexus). At minimum, 70% of these myenteric neurons are part of a heterogenous population of cholinergic neurons, while markers such as nitric oxide synthase are present in inhibitory neurons of smooth muscle as well as interneurons [35]. There is no definitive cross species marker for IPANs, but calbindin mark these neurons in the guinea pig ENS, while in mice these can also stain for calretinin [35, 36]. GABA and dopaminergic neurons are also detected, but their precise roles in ENS functions remains elusive and their synaptic targets are unknown [35, 37].

In the submucosal ganglia, murine ileum studies have shown that there are three major populations; 51% vasoactive intestinal peptide positive (VIP), 41% choline acetyltransferase positive (ChAT), and the remaining 8% of neurons express neither marker [38]. These VIP neurons can express neuropeptide Y (NPY) and tyrosine hydroxylase, while calretinin positive cells represent over 90% of neurons, including those that are VIP positive [35, 38]. As with the myenteric plexus, the population percentages shift depending on the species; in humans, VIP positive neurons account for 40% and substance P (SP) positive neurons account for 42% – comparative studies between canine and human submucosal plexi of the jejunum showcase 30% SP positive neurons in canine tissue, indicating that there is neuroanatomical evidence for the potential of different functions for each of these cell types in various species [39].

REGULATING HOMEOSTASIS AND THE MICROBIOME

Alterations in neuron density contribute to the intensity of intestinal inflammation [40]. Enterocolitis significantly reduces the quality of life for many people that experience adverse symptoms such as fever and emesis [15, 41].

Inflammation in the intestine can be caused by an assortment of maladies. One of the more notable of these is inflammatory bowel diseases (IBD), which includes ulcerative colitis (UC) and Crohn's disease (CD) [42]. As structural abnormalities have been shown in the ENS in association with IBD, the role the ENS plays in these disease profiles should be further explored [43].

Regulation of homeostasis within the intestinal tract is paramount for microbiota health, as certain members of this group such as the diarrhoeal pathogen Clostridium difficile can cause harm when left unregulated [12, 44]. Some of the main components of the adult microbiota are *Faecalibacterium prausnitzii*, *Roseburia intestinalis* and *Bacteroides uniformis*, though the specific activities of these species are largely unknown, and in some individuals they are significantly less prevalent [45]. Some members to the *Lachnospiraceae* class of microbes, including *E. hallii* and *Anaerostipes spp.*, are known to be able to use lactate and acetate to produce metabolite butyrate which might be involved in anti-inflammatory signaling [46]. These connections implore us to delve further into metabolites that may produce pro or anti-inflammatory effects within host tissue utilizing human *in vitro* tissue models.

SPECIFIC AIMS

The human gastrointestinal tract is in continuous contact with nutritional content, metabolites, and the microbiome, yet there are limited systems to study the interplay between the enteric nervous system (ENS) and the various functions and inhabitants of the mature GI tract. We proposed to establish a system to study signaling of the ENS in mature human cells. Our hypothesis was that 3D intestinal scaffolds, with the ability to house bacterial content, may by readily integrated with human induced neural stem cells to form an *in vitro* ENS (ivENS). The *goal* of this work was to develop an *in vitro* ENS tissue model utilizing human derived cells, capable of long term culture, to mimic endogenous ENS function, in both healthy and diseased states. This adaptable system should be suitable for biological, therapeutic, and regenerative applications. Utilizing this technology, our *long-term goal* is to create a simple and effective tissue model system to study the gut-brain axis, and to create a hospitable system to understand microbial interactions and communication. To accomplish this goal, we have proposed the following aims:

Aim 1: **Develop and characterize an *in vitro* enteric nervous system tissue model utilizing human derived cells.**

The *objective* of this aim is to incorporate neural functionality by adding human induced neural stem cells (hiNSCs) onto the perimeter of intestinal scaffolds containing human intestinal myofibroblasts (IMF) in order to mimic the location of endogenous neural plexi in relation to the lumen. The growth of hiNSCs will be guided utilizing neural growth factor (NGF), which is incorporated into the scaffold bulk prior to neural seeding. Scaffold viability will be tested using Live/Dead assay, and Alamar Blue assay will be used to quantify tissue metabolism. Immunofluorescence will be used to visualize the locations and phenotypes of the various cell types within the scaffolds. Neuronal marker beta III tubulin (TUJ1), neuronal nitric oxide synthase (nNOS), tight junction protein marker (ZO1) will be visualized using these techniques. Transcription factors Muc-2, Muc5AC, tachykinin 1 (Tac1), neurokinin receptor 1 (NK1) levels will be determined utilizing quantitative RT-PCR to determine that respective cell functionalities are maintained within the scaffolds following combined culture. From this analysis, we can determine the completion of this aim through sufficient innervation and ENS function of the ivENS model. To do so, the system will need to show, <u>infiltration of the hiNSCs</u> into the bulk of the scaffold, <u>expression of biomarkers</u> indicating that relevant cell types are present (TuJ1, nNOS, and ZO-1), <u>transcription of genes</u> of interest are expressed (Muc-2, Muc5AC, Tac1, and NK1), and <u>survival</u> past 4 weeks of culture.

<u>Aim 2:</u> **Incorporate microbial metabolites within the *in vitro* ENS to assess inflammatory response.**

The <u>*objective*</u> of this aim is to perturb the ivENS model utilizing metabolites associated with the endogenous microbiome to evaluate the tissue response to external stimuli to determine whether they elicit a pro or anti-inflammatory signal.

We will trigger inflammation utilizing lipopolysaccharides (LPS) from *E. coli* and monitor the response of the ivENS. From this analysis, we will indicate the completion of this aim through sufficient ability for the model to undergo an inflammatory response and to produce both epithelial, and neural, indicators of that response. To do so, the system will need to show, production of proinflammatory cytokines (IL-8, IL-6, MCP-1, IL-1β, and TNF-α) and production of Substance P by the neurons.

CHAPTER 2 : DEVELOPMENT AND CHARACTERIZATION OF IN VITRO ENTERIC NERVOUS SYSTEM SCAFFOLDS

Adapted from manuscript authored by Eleana Manousiouthakis, Ying Chen, Dana Cairns, Rachel Pollard, Kaia Gerlovin, Michael Dente, Yasmin Razavi, David L. Kaplan [47].

Contributions: EM, YC, DC, and DK designed and conceived the study. EM, DC, RP, KG, MD, and YR conducted the experiments and acquired the data. EM, YC, DC, RP, and MD contributed to analysis and interpretation of the data. EM, RP, KG, MD, and YR drafted the article, with the contribution and critical revision of all authors. All authors approved the final version of the manuscript.

ABSTRACT

Bidirectional interactions between the human central nervous system and the gastrointestinal tract (GI), via the enteric nervous system, are unmapped and central to many human conditions. There is a critical need to develop 3D human *in vitro* intestinal tissue models to emulate the intricate cell interactions of the human enteric nervous system within the GI tract in order to better understand these complex interactions that cannot be studied utilizing *in vivo animal models*. *In vitro* systems, if sufficiently replicative of some *in vivo* conditions, may assist with the study of individual cell interactions. Here we describe a 3D innervated tissue model of the human intestine consisting of human induced neural stem

cells (hiNSCs) differentiated into relevant enteric nervous system neural cell types. Enterocyte-like (Caco-2) and goblet-like (HT29-MTX) cells are used to form the intestinal epithelial layer, and intestinal myofibroblasts (IMF) are utilized to simulate the stromal layer. *In vitro* enteric nervous system (ivENS) cultures supported survival and function of the various cell types, with mucosal and neural transcription factors evident over 5 weeks. The hiNSCs migrated from the seeding location on the peripheral layer of the hollow scaffolds toward the luminal epithelial cells, prompted by the addition of neural growth factor (NGF). nNOS-expressing neurons and the substance P precursor gene TAC1 were expressed within the ivENS system to support the utility of the tissue model to recapitulate enteric nervous system phenotypes. This innervated tissue system offers a new tool to use to help in understanding neural circuits controlling the human intestine and associated communication networks.

1 INTRODUCTION

The intestine is a vital organ able to perform secretory, motor, and absorptive functions within the body [48]. Within the intestine, the intrinsic neural architecture was first discovered when the tissue was able to continue motor activity following severing of the connection to the CNS [34]. The ENS has since been described as a "second brain" due to its ability to interact with the central nervous system (CNS) and to broadly impact human health. The complex circuitry of the ENS controls a variety of known gut functions encompassing motility, secretion, vascular tone, and release of hormones [49]. These key functions suggest the need for in depth studies of the adult human ENS, yet current options to assess intestine neuromodulation are primarily limited to animal studies, 2D cell culture studies, and organoids [8, 16]. All of these systems have inherent limitations towards an understanding of the ENS. Differences in the development between human and animal intestinal systems, the lack of microbiome interplay, and developmental immaturity of the in vitro systems vs. the adult homeostatic state of the intestine, all effect the versatility of these systems when exploring the interactions between the enteric nervous system and the lumen of human patients [8, 20, 50]. The enteric nervous system develops differently contingent on the specie of animal. Concepts such as intrinsic mucosal reflex pathways [51, 52], which directly affect the response to luminal content, are also different. For example, in the GI tract of smaller mammals, 97% of traced myenteric neurons are assumed to be primary afferent (respond to luminal chemistry via processes in the mucosa) in nature, but in larger mammals the number of primary afferent neurons represents a minority of traced neurons (less than 30%) [51, 53].

Human cells and tissues to help elucidate the roles of the complex cell types comprising human intestinal tissues are essential to develop relevant treatment strategies for various human diseases. 2D cell co-culture systems have helped to elucidate many mechanistic interactions between intestinal epithelial cells and components of the enteric nervous system, such as the presence of neuronal serotonin transporter (SERT) in human intestinal epithelial Caco-2 cells [54]. However, these 2D systems are unable to recapitulate the 3D microenvironment which has been shown to provide geometric tunability for cellular cultures, mimicking physiological conditions and altering cellular functions to better mimic endogenous systems [10, 26, 55].

Intestinal organoid systems have been crucial to the study of the ENS in a 3D environment and contain cells derived from all three germ layers (endodermal intestinal epithelium, mesodermal mesenchyme, and ectodermal neural crest-derived cells) [8, 56]. Unfortunately, these systems usually mimic fetal stages of development and only recapitulate fully mature cells when the organoids are transplanted in vivo [56, 57]. These limitations are often compounded with necrosis and lack of compartmentalization with culture time. As more neurodegenerative disease interactions with the ENS are explored, many of which are associated with advanced age, systems that mature fully *in vitro* are needed [58-61]. Unlike animal models, 2D cell culture, and organoid cultures, 3D tissue engineered systems can harness the properties of endogenous adult human systems in a modular, compartmentalized design in the form of complex *in vitro* models with sustainable cultivation *in vitro*.

To address the above needs, the goal in the present study was to develop a physiologically relevant *in vitro* human intestine model to study neuromodulation at the gastrointestinal level utilizing silk based scaffold. Silk systems have shown their ability to sustain long term *in vitro* cultures (8 months) making this protein an ideal candidate for scaffold material [33]. We focused on the development of *in vitro* 3D human innervated intestine tissue model utilizing silk protein that integrates human induced neural stem cells (hiNSCs) differentiated into relevant enteric nervous system neural cell types, and intestinal myofibroblasts (IMF) to provide support of the enterocyte-like (Caco-2), and goblet-like (HT29-MTX) cells that form the intestinal epithelial layer of the lumen [10, 23]. The system co-localizes these cell populations in physiologically relevant locations. IMFs are localized under the epithelial layer to the submucosal area of the scaffold, to secrete growth factors that support epithelial health [62]. hiNSCs are localized to the surrounding wall of the scaffold and allowed to infiltrate into the submucosal area, similar to endogenous patterning of the submucosal plexus of the ENS, in order to control a myriad of epithelial function, including barrier and secretory functions [2, 9, 63] [64]. The multimodal nature of our system allows for each cell type to be replaced or interchanged with cell populations from various source populations while maintaining 3D architecture [65]. Unlike our previously reported systems, where we have confirmed the ability to support microbial communities [10], this system adds capability for long term human enteric neural culture alongside our established epithelial layer, to further expand the biological relevance and the questions that we can probe with the system.

2 METHODS

2.1 Silk scaffold generation

Scaffolds were constructed according to previous work [24] [10]. In brief, molds were formed utilizing Sylgard 184, Polydimethylsiloxane (PDMS, Dow Corning, Midland, MI), following the established protocol [10]. Teflon-coated stainless-steel wires (McMaster-Carr, Elmhurst, IL) were utilized to form the hollow tube of the scaffolds. Molds can be recovered after each process for future silk solution casting. Silk solutions prepared from 30-minute extraction to remove sericin were between 5-6% protein and used to form scaffolds. Post pouring the silk solution into the molds, the scaffolds were frozen at -20°C and lyophilized the following day. In order to induce beta sheet formation, lyophilized scaffolds were autoclaved. Scaffolds were then hydrated in diH_2O overnight and trimmed to 8x5x5mm. Trimmed scaffolds were placed in diH_2O, autoclave sterilized, and stored at room temperature until used.

2.2 Cell Culture

2.2.1 Cell sources: The human intestinal epithelial cells, Caco2 and HT29-MTX, were obtained from ATCC (Rockville, MD) and from the Public Health England Culture Collection (Salisbury, Great Britain), respectively. These were cultured in DMEM supplemented with 10% fetal bovine serum, 10 µg/mL human transferrin (Gibco, Gaithersburg, MD), and 1% penicillin/streptomycin. Human Intestinal Myofibroblasts (IMF) (Lonza, Portsmouth, NH) were cultured in SmGM™ Bullet Kit. For Caco-2 and HT29-MTX, cells from passage number 38–50 were used for cultures, and for IMF, passage number 3–5 were used.

Human induced neural stem cells (hiNSCs) were generated as previously described [23]. Briefly, human foreskin fibroblasts (HFFs) were plated at a concentration of 10^5 cells in one well of a 6-well plate, and cultured in fibroblast media (DMEM, 10% FBS, and 1% antibiotic-antimycotic). Concentrated aliquots of polycistronic lentivirus expressing OCT4, KLF4, SOX2, and cMYC (Addgene #24603, a gift from Jose Cibelli) were used to infect HFFs in fibroblast medium with polybrene (Millipore) at a multiplicity of infection (MOI) = 1-2. Media was changed to hiNSC media: Knockout (KO) DMEM supplemented with 20% KO xeno-free serum replacement, 20 ng/mL recombinant bFGF, 1% Glutamax, 1% antibiotic-antimycotic, and 0.1 mM β-mercaptoethanol which also contained 1% KO growth factor cocktail (GFC) (Invitrogen). Four days later, cells were trypsinized and plated onto mouse embryonic fibroblast (MEF) feeder layers that had been inactivated by mitomycin C. hiNSC media (without KO-GFC) was subsequently changed every 1-3 days. At day 30 or later, colonies were mechanically picked and passaged onto fresh feeder MEF plates. Each colony represented one hiNSC line. hiNSCs were enzymatically passaged as colonies using trypsin-like enzyme, TrypLE (Invitrogen), expanded, and subsequently frozen to make stocks. All generated lines tested negative for mycoplasma contamination.

Human Induced Neural Stem Cells (hiNSCs) used for seeding, were cultured in KO medium (knockout (KO) DMEM supplemented with 20% KO xeno-free SR, 20 ng/mL recombinant bFGF, 1% Glutamax, 1% antibiotic-antimycotic, and 0.1 mM β-mercaptoethanol) [23]. Colonies of hiNSCs were cultured on mouse embryonic fibroblast cells (MEF) (ATCC, Rockville, MD) feeder layers until time of differentiation. Differentiation toward neural phenotype was performed by transferring hiNSCs from colonies onto gelatin coated plates and removing the fibroblast growth factor from the KO medium for 7 days of culture, at which point cells were trypsinized and added to the scaffolds alongside the intestinal cells as described in the seeding protocol. All cells were maintained in a humidified chamber at 37°C with 5% CO_2.

2.2.2 Cell seeding on silk scaffolds: The human epithelial cells (Caco2 and HT29-MTX) were used to coat the inside of the scaffold lumen at a 3:1 ratio of Caco2:HT29-MTX, with $2x10^6$ cells/mL. The human intestinal myofibroblasts (IMF) were used in the porous bulk space of the scaffold at a concentration of 1×10^6 cells/mL. Collagen solution with neural growth factor 50 ng/mL (NGF, R&D Systems, Minneapolis, MN), 80% rat-tail collagen (2.05mg/mL in 0.6% Acetic Acid, First Link, UK), 10% 10X DMEM, and 10% 1X DMEM, was prepared in order to maintain the human intestinal myofibroblasts in the spongy bulk space of the scaffolds and provide guidance for neural innervation into the scaffold bulk. The myofibroblast cells and epithelial cells populated the scaffolds for 1 week prior to hiNSC seeding.

hiNSCs were differentiated toward neural linage for 1 week prior to seeding on scaffolds. Following differentiation, hiNSCs were removed from gelatin plates using TrypLE™ Select Enzyme (1X) (ThermoFisher, Waltham, MA) and were suspended in collagen solution, 80% rat tail collagen (2.05mg/mL in 0.6% Acetic

Acid, First Link, UK), 10% 10X DMEM, and 10% 1X DMEM, without NGF and coated on the peripheral edge of the mature scaffolds (Figure 1, b9). The four conditions studied included: (a) intestinal cells only (Caco-2, HT29-MTX, and H-InMyoFib), (b) hiNSCs only, (c) co-culture (all listed cell types), and (d) cell free scaffolds. All scaffolds were cultured in a 1:1 ratio of 1xDMEM and SmGM, supplemented with 50ng/mL of NGF and 0.2% primocin (Invivogen, San Diego, CA).

Systems with both epithelial cells and IMFs were cultured for 7 days prior to hiNSC seeding. During this time, hiNSCs from expansion cultures were differentiated toward neural linage in medium without fibroblast growth factor (FGF) for 7 days [23]. Following differentiation, hiNSCs were seeded at $1x10^6$ cells/100µL, with 25µL cell suspension collagen solution seeded on each side of the perimeter of the scaffold. Collagen was allowed to gel for 10 minutes per side of the ivENS scaffold (**Figure 2-1**, b9). Prior to hiNSC seeding, during the initial intestinal myofibroblast seeding, NGF was incorporated into the collagen solution that fills the bulk of the scaffold to promote guidance following seeding on the perimeter of the scaffold.

(a)

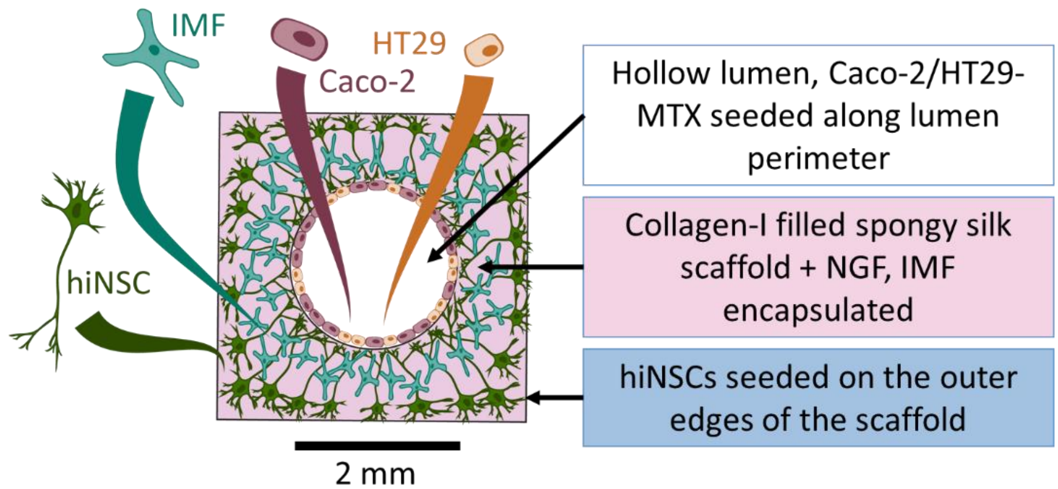

(b)

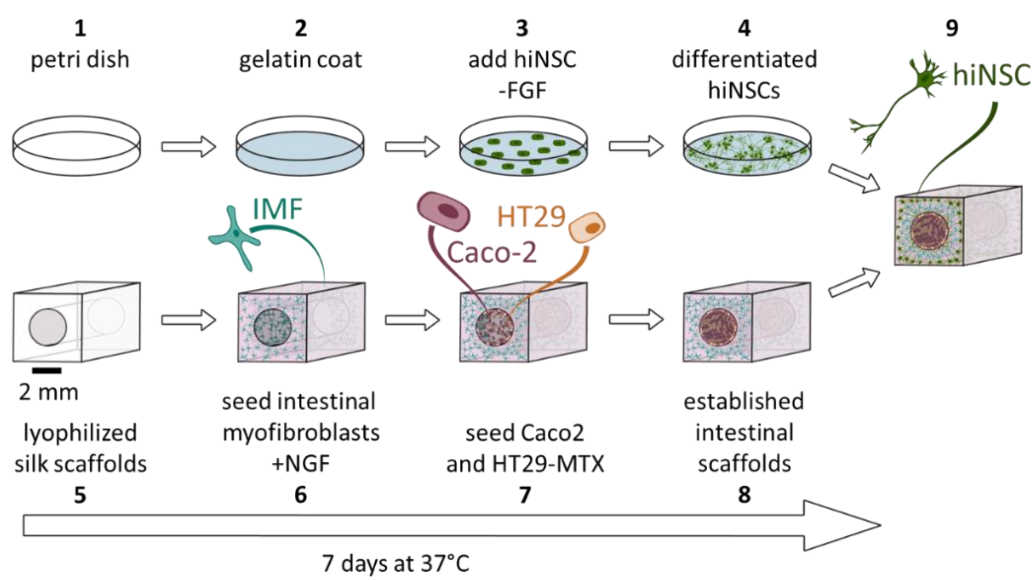

Figure 2-1: Schematic. (a) Schematic indicates a cross section of the ivENS with the location of the various cell types within the mature ivENS. Porous silk sponges were filled with collagen-I encapsulating Intestinal Myofibroblasts (IMF) and Neural Growth Factor (NGF). Following collagen-1 gelation, epithelial cells Caco-2 and HT29-MTX were seeded within the lumen of the scaffold. After 7 days, differentiated human induced neural stem cells (hiNSCs) were added to the perimeter of the scaffolds. (b) Process Flow time line for ivENS cell seeding, cell cartoons indicate the point in the process and location each cell type was seeded during scaffold preparation. Samples were collected at weekly time points, following hiNSC seeding unless otherwise noted in the methods.

2.3 Immunostaining

2.3.1 Sample Preparation: Samples utilized for immunostaining were rinsed three times with 1x DPBS, and fixed with 4% paraformaldehyde (PFA, Santa Cruz, CA). All scaffolds were then permeabilized using 0.1% Triton X-100 in phosphate-buffered saline (PBS, Invitrogen), then blocked with 5% bovine serum albumin (BSA, Sigma-Aldrich, Natick, MA) and 2% Donkey Serum for 2 hours. Primary antibodies were incubated overnight at 4°C with the dilutions in Table S1. Samples were then rinsed and immersed in secondary antibodies with the dilutions in **Table 2-1**, and counterstained with dihydrochloride (DAPI, Invitrogen) prior to imaging.

Excised intestines from chick embryos were wholemount immunostained with Human nuclear stain (HN) Antibody, clone 235-1, Cy3 conjugate (Millipore, Darmstadt, Germany), β-Tubulin III (Sigma-Aldrich, Natick, MA), and DAPI (ThermoFisher, Waltham, MA). Wholemount staining was performed following an overnight fix in 4% paraformaldehyde. Samples were then permeabilized using 0.1% Triton X-100 in phosphate-buffered saline (PBS, Invitrogen), then blocked with 5% bovine serum albumin (BSA, Sigma-Aldrich, Natick, MA) in 0.1% Triton X-100 in 1xDPBS for 2 hours. Primary antibodies were incubated overnight at 4°C with the dilutions in **Table 2-1**. Samples were then rinsed and immersed in secondary antibodies with the dilutions in **Table 2-1** and counterstained with dihydrochloride (DAPI, Invitrogen) for 3 hours at room temperature. Samples were washed with 1xDPBS 3 times for 10 minutes each prior to imaging. The 3 samples injected with hiNSCs in the neural tube and 3 control (sham surgery) samples were then imaged using confocal microscopy on a Leica SP8.

Table 2-1: Immunostaining Antibody Dilutions.

Antibody	Catalogue Number	Dilution
Rabbit Anti-β-Tubulin III antibody	T2200	1:500
Rabbit Anti-nNOS (neuronal) antibody [EP1855Y]	ab76067	1:200
Mouse Anti-Human ZO-1 Clone 1/ZO-1 (RUO)	610966	1:500
Mouse Anti-Nuclei Antibody, clone 235-1, Cy3 conjugate (HN)	MAB1281C3	1:200
DAPI (4',6-Diamidino-2-Phenylindole, Dihydrochloride)	D1306	1:1000
Donkey anti-Mouse IgG (H+L) Secondary Antibody, Alexa Fluor® 594 conjugate	A-21203	1:500
Donkey anti-Rabbit IgG (H+L) Secondary Antibody, Alexa Fluor® 488 conjugate	A-21206	1:500

2.3.2 Cryosectioning: Samples processed for cryosectioning were rinsed three times with 1x DPBS, and fixed overnight with 4% paraformaldehyde (PFA, Santa Cruz, CA). Scaffolds were rinsed with 1xDPBS, 10% sucrose-PBS for 2 hours at room temperature, then allowed to equilibrate in 30% sucrose-PBS solution overnight at 4°C. Scaffold solution was replaced with 1:1, 30% sucrose-PBS solution and optimal cutting temperature compound (OCT compound) and incubated overnight at 4°C. Scaffolds then placed in OCT solution overnight at 4°C and embedded in fresh OCT the following day. Scaffolds were stored at -80°C until sectioning. Scaffolds were sectioned at 50μm using a Leica CM 1950 cryostat.

2.4 RNA isolation

Following culture, in order to isolate components from the hiNSCs and cell types localized to the bulk of the scaffold, all samples were rinsed three times with 1x DPBS and flash frozen in microcentrifuge tubes in a liquid nitrogen bath. Scaffolds were then stored at -80°C. These frozen scaffolds were submerged in lysis buffer, cut with scissors, and homogenized using a Fisherbrand™ 150 Handheld Homogenizer Motor (Fisher Scientific, Pittsburgh, PA). Once cells are lysed from the freezing process and homogenized to assist with the release of cellular components from the silk scaffold, an AllPrep, DNA, RNA, and protein extraction kit (Qiagen, Germantown, MD) was used to collect the mRNA in each of the scaffold samples following the manufacturer's instructions. Concentration and purity of mRNA was measured using the ThermoFisher NanoDrop 2000.

2.5 Mucosal screening via Quantitative RT-PCR

Quantitative RT-PCR was performed to quantify the expression of ENS mucosal and substance P (SP) cascade markers in mono-culture and co-culture silk scaffolds. The mRNA was isolated from samples using the aforementioned method. The mRNA samples were then reverse transcribed to cDNA using the High Capacity Reverse Transcription kit (ThermoFisher, Waltham, MA) in 20 μL reactions containing 400 ng of mRNA, according to the manufacturer's instructions. Amplification was carried out as follows: 10 minutes at 25℃, 120 minutes at 37℃, and then 5 minutes at 85℃.

Quantitative RT-PCR was performed using Taqman fluorescent hybridization probes (ThermoFisher, Waltham, MA) according to the manufacturer's instructions. The reactions were incubated at 95 ℃ for 10 min followed by 2 min at 50℃. Amplification was then carried out with 50 cycles of 15 seconds at 95℃ and 1 min at 60 ℃. Samples with Ct values higher than 40 cycles were counted as no expression. Relative mRNA expression was then calculated using a comparative cycle threshold method (ΔΔCt). All genes and experimental groups were normalized using 18S as a housekeeping gene. Mucosal markers used include Muc-2 and Muc5AC, and substance P cascade markers include TAC1 and NK-1.

2.6 Alamar Blue Assay

Alamar blue was used to measure the metabolic activity of each of the scaffold conditions. A 10% alamar blue solution was made in a one to one ratio of SmGM and DMEM medium and incubated with the samples for 1 hour at 37°C. Following incubation, samples were read on a plate reader in triplicate. The scaffolds were then placed in tubes and frozen for RNA, DNA, and protein extraction. Data was collected from 3 biological replicates.

2.7 Live Imaging Viability Assay

Viability was determined utilizing Calcein, AM, cell-permeant dye (ThermoFisher, Waltham, MA) on endpoint samples. Calcein, AM was performed per manufacturer's instructions.

2.8 Microscopy

Fluorescent images of sectioned slides and live staining were obtained using a Keyence BZ-X700 microscope and associated software. Images of wholemount immunostained chick intestine were taken using confocal fluorescence microscopy using a Leica SP8 (Wetzlar, Germany) and associated software.

2.9 hiNSCs chick migration assay

Single cell suspension hiNSCs were injected into the developing neural tube at embryonic day 3 (E3) following our previous protocol [23]. Embryos were harvested and fixed with 4% paraformaldehyde at E12-E14 of gestation post-injection for subsequent analysis.

2.10 Statistics

Two-Way ANOVA with Tukey test was applied in the comparison between multiple experimental groups, as well as cell free control for alamar blue analysis over time. All data are expressed as mean ± standard deviation. A p-value less than 0.05 was used to determine significance. One-Way ANOVA with Tukey test was applied to each gene for quantitative RT-PCR. All data are expressed at fold change mean ± standard deviation. A p-value less than 0.05 was used to determine significance. All statistical analysis was carried out using GraphPad Prism 7 software (GraphPad Software, CA, USA).

3 RESULTS

3.1 Preparation and design of ivENS scaffolds

In order to recapitulate the properties of the endogenous adult human gastrointestinal enteric nervous system in a modular, compartmentalized design (Figure 2-1, a), we prepared spongy silk scaffolds featuring a hollow lumen capable of housing gastrointestinal cells according to our previous protocol [10]. Our design needed interconnected pores in order to allow human induced neural stem cells seeded on the outside edges of the scaffolds to infiltrate towards the lumen. Thus, the established porous silk scaffold system for intestinal engineering was utilized [10]. This system allows the cells to be seeded in isolation within different compartments of the system, but provides the infrastructure for cell interaction as the varied cell types grow in the matrices (Figure 2-1, b). The ivENS systems were engineered by first culturing primary human intestinal myofibroblasts (IMF) within the scaffold bulk space along with neural growth factor (NGF) and human intestinal epithelial cells (Caco-2 and HT29-MTX cells) on the surface of the lumens in the silk scaffolds.

3.2 Migration of hiNSCs from neural tube to the gastrointestinal tract in vivo

We tested the neural crest cell behavior of the hiNSCs in order to determine whether they would follow a migratory path similar to endogenous ENS cells and differentiate into neurons. Injection of hiNSCs into the neural tube of chick embryos were performed at embryonic day 3 (D3) (Figure 2-2, a). Intestinal tissue samples were collected at embryonic day 12-14 (D12-D14) (Figure 2-2, b) immunostained. D12-D14 chicks that had sham surgery performed did not stain for human nuclear stain (HN) cells in the GI wall (**Figure 2-2**, c, d). Samples that were injected with hiNSCs stained positive for HN, which indicated cells of human origin, and the NH+ cells migrated into the gastrointestinal wall of D12-D14 chicks (**Figure 2-2**, e, f). Thus, hiNSCs responded to migratory cues in vivo (**Figure 2-2**).

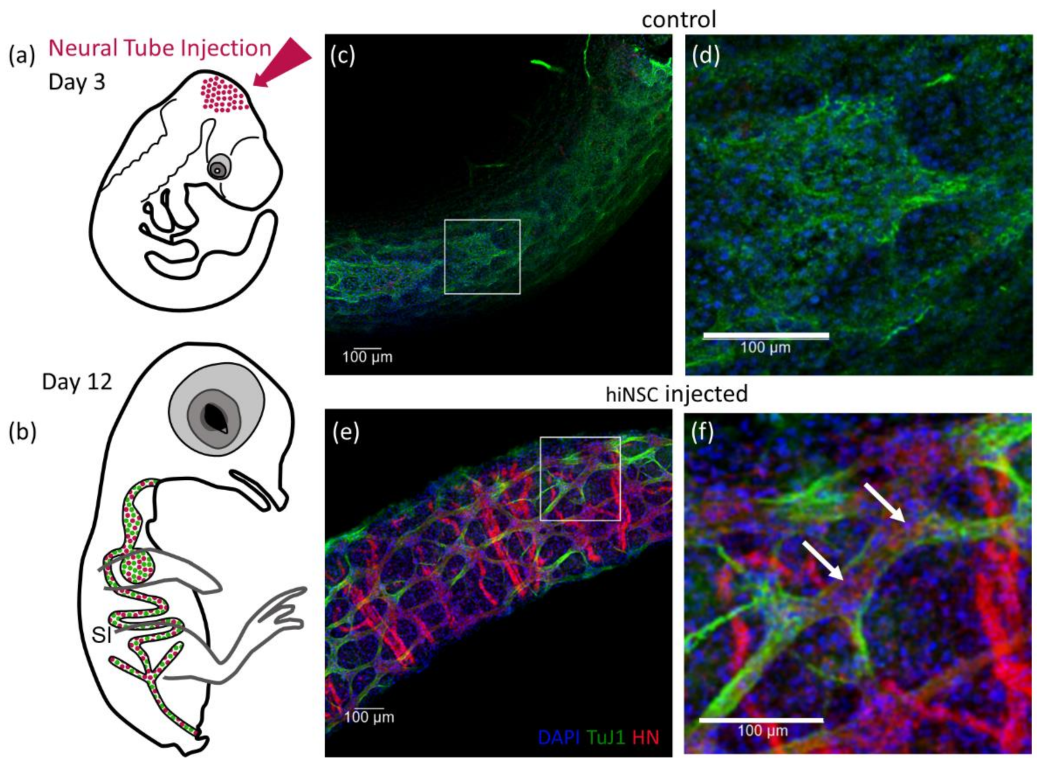

Figure 2-2: Chick migration assay indicates the response to endogenous neural crest migratory cues. At day 3 (D3) of gestation, hiNSCs (magenta dots) were injected into the neural tube of chick embryos (a). Neural crest cells invade the foregut and migrate caudally to populate the gut during development, samples are collected following day 12 of gestation when both the hiNSC derived ENS (magenta dots) and endogenous neural crest derived ENS (green dots) have made their complete migration past the small intestine (SI)(b). 3D confocal image stack max projection of whole mount immunostained representative images of D12-D14 chick intestine following control (c, d) or hiNSC injection (e, f). Human nuclear stain, HN (red) indicates nuclei of cells of human origin, thus indicating hiNSCs. Pan neuronal marker beta III tubulin TUJ1 (green) and nuclear stain DAPI (blue). White arrows indicate human nuclear stain within TuJ1 positive nerve bundles. Control is a sham surgery without hiNSC injection. Scale bars 100 µm.

3.3 Long-term scaffold viability

Following the combination of all cell types within the in vitro enteric nervous system (ivENS) scaffolds, the cells remained metabolically active for at least 3 weeks, based on Alamar Blue assay (**Figure 2-3**). At weeks 1, 2, and 3, all scaffolds had significantly higher levels of metabolic activity compared to cell free scaffold controls, showing that cells present within each system remained metabolically active over time allowing for sustained cell function. At week 3 hiNSC only scaffolds had a significantly higher level of metabolic activity compared to both intestinal only scaffolds and co-culture scaffolds. There was no statistical difference between cell seeded groups in weeks 1 and 2. Cell survival within the ivENS was confirmed using live staining of Calcein AM (**Figure 2-4**).

In order to determine how long the hiNSC survive in intestinal cell culture conditions, the hiNSC, Caco-2 and HT29-MTX cells were cultured within the scaffolds in DMEM:SmGM medium; Scaffolds were trimmed in half along the lumen in order to better visualize the cell infiltration into the bulk of the scaffold (**Figure 2-4**, a). Survival of the hiNSCs within the bulk was determined out to at least 60 days in culture as shown by Calcein AM (**Figure 2-4**, b-d). The hiNSCs survived in the scaffolds and had infiltrated through the bulk (B) of the scaffold, toward the lumen (LS) from the initial seeding location at the perimeter of the scaffold on the outer side (OS).

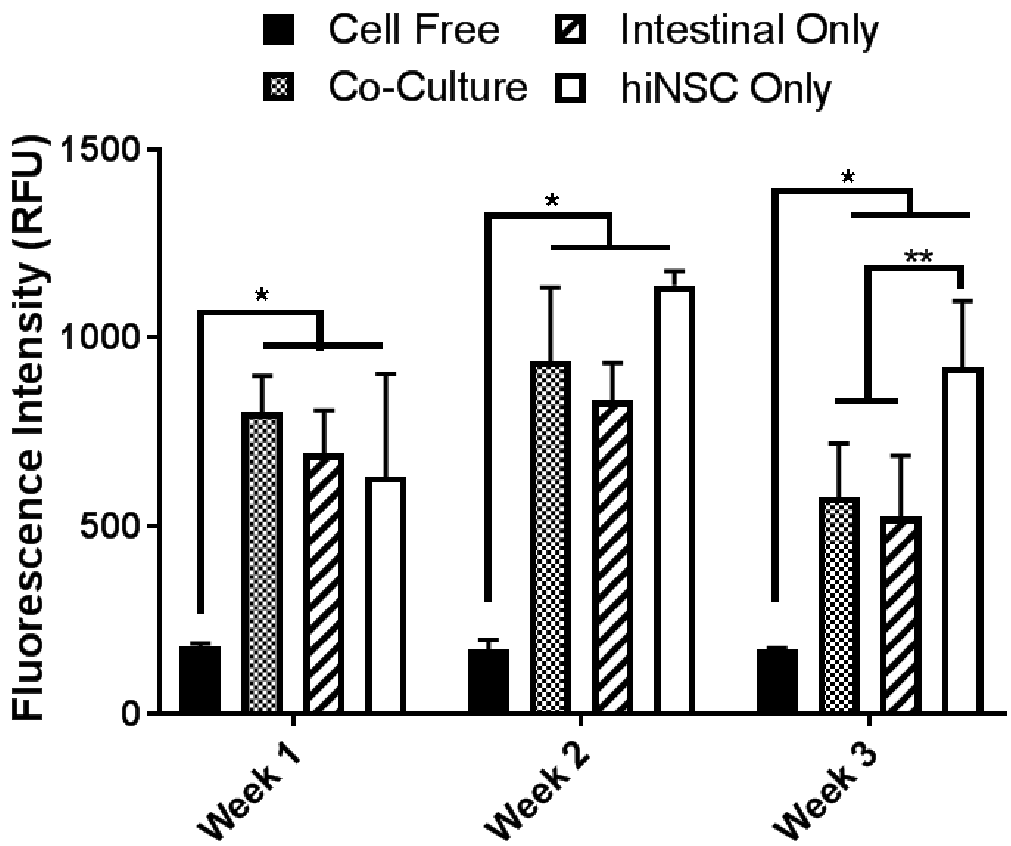

Figure 2-3: Alamar Blue viability within ivENS scaffolds. Alamar Blue cell viability assay was used to determine cell survival. Scaffold metabolic activity was assessed over 3 weeks. At weeks 1, 2, and 3, all scaffolds had significantly higher levels of metabolic activity compared to cell free scaffold controls, showing that cells present within each system remained metabolically active over time. At week 3 hiNSC only scaffolds had a significantly higher level of metabolic activity compared to both intestinal only scaffolds and co-culture scaffolds. There was no statistical difference between cell seeded groups in weeks 1 and 2. * P<0.05 relative to scaffolds with no cells added. ** P<0.05 relative to week 3 hiNSC only scaffolds. The mean ± standard deviation of fluorescence, based on 3 independent biological replicates.

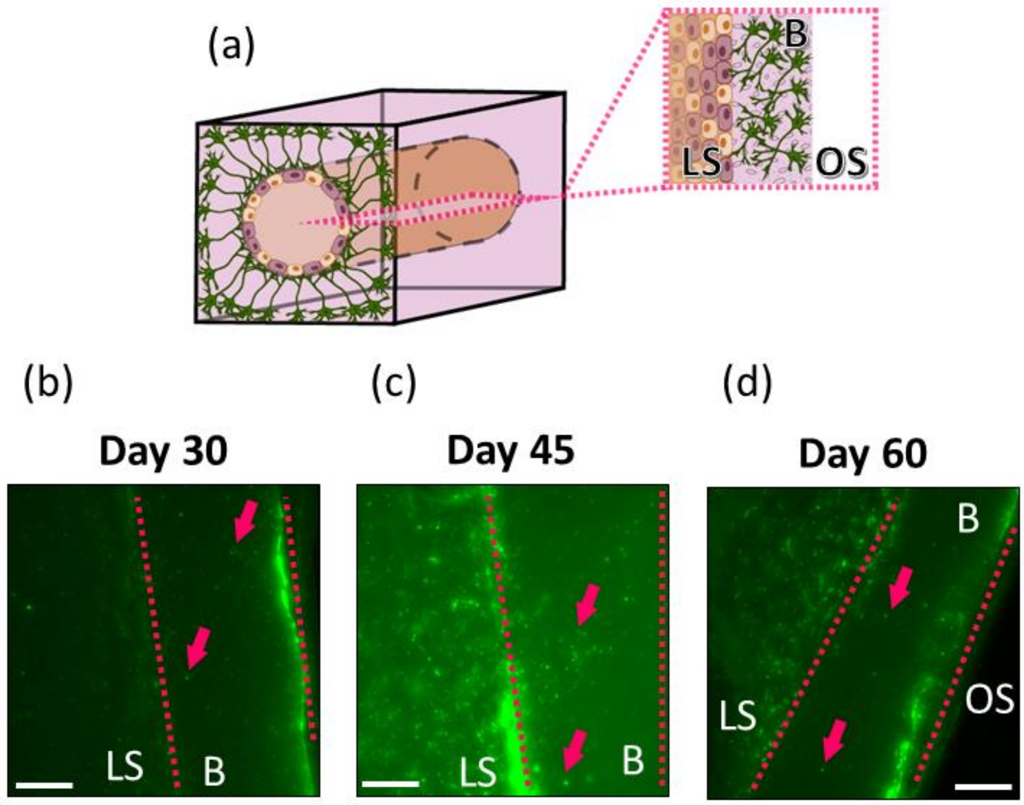

Figure 2-4: Live staining within ivENS scaffolds. Scaffolds were cut through the bulk (B) of the scaffolds on both sides to expose the cells seeded within the bulk as well as on the luminal surface (LS) for imaging (a). Schematic of the scaffold (a) shows Caco-2 (red) and HT29-MTX (orange) on the luminal surface, and hiNSCs (green) within the trimmed bulk (B) region. Scale bars 500 µm. Scaffolds seeded with hiNSCs and Caco-2/HT29-MTX after day 30 (b), day 45 (c), and day 60 (d) were live stained with Calcein-AM viability dye (green). Images show cross section of the bulk of the scaffold (B) and the luminal surface of the scaffold (LS) for each time point, indicating cells were successfully delivered onto the silk scaffold perimeter and infiltrated into the scaffold bulk toward the lumen (magenta arrows). The outer surface (OS), where the hiNSC are originally seeded, can be seen in frame at day 60 showing some cells remain at the perimeter out to this time point.

3.4 Enteric Nervous System Neural Differentiation and Function

Differentiation status can be determined by the presence of characteristic markers of endogenous enteric nervous system neural subtypes. Histological examination of neuronal markers in ivENS scaffolds cultured for 3 weeks indicated expression of TuJ1 and nNOS in neurons cultured within the system. Sections that were 50µm thick spanned the width of the scaffold wall, from the lumen to the exterior surface where initial hiNSC seeding occurred. The location of neurons throughout the stained sectioned ivENS confirmed the data shown in the Calcein AM staining (**Figure 2-4**, b-d), that neurons migrated from the periphery or outer surface (OS) toward the luminal surface (LS) (**Figure 2-5**, b, d). Epithelial cells present on the luminal surface expressed the tight junction marker ZO-1 (**Figure 2-5**, b). Co-cultured ivENS systems expressed enteric nervous system neural subpopulations, neuronal nitric oxide synthase+, at week 3 of culture (**Figure 2-5**, d).

In order to explore functionality of the co-culture system, scaffold mucus transcription was assessed via quantitative reverse transcription-polymerase chain reaction (qRT-PCR) (**Figure 2-6**). As expected, cell free scaffolds did not yield any mRNA during the AllPrep extraction and thus were not utilized in the analysis. Scaffolds were collected at week 5 to assess gene expression. Gene expression levels of two intestinal epithelial mucosal markers, including Muc-2 and Muc5AC were detected in both intestinal only and co-culture scaffolds. Muc-2 expression was upregulated in co-culture scaffolds compared to intestinal only scaffolds (**Figure 2-6**, a). Muc5AC expression was maintained in co-culture scaffolds compared to intestinal only scaffolds (**Figure 2-6**, b). Expression of Tac1, a gene that encodes for tachykinin peptide family including substance P (SP), was seen in co-culture scaffolds at week five (**Figure 2-6**, d). For the neurokinin 1 (NK1), a SP receptor, expression, Ct values of the intestinal scaffolds either yielded "No Ct" or cycle values over 40 (**Table 2-2: Delta Ct values using 18S as housekeeping.**). For NK1, hiNSC only, but not co-culture scaffolds were significantly different from the intestinal only scaffolds (**Figure 2-6**, c).

Table 2-2: Delta Ct values using 18S as housekeeping.

	Muc-2	Muc5AC	NK1	TAC1
hiNSC only	19.28 ± 2.91	15.22 ± 3.34	24.65 ± 1.62	18.22 ± 0.78
intestine only	18.78 ± 0.88	12.40 ± 0.41	†32.08 ± 1.40	27.46 ± 2.89
co-culture	17.21 ± 0.39	12.55 ± 0.41	28.02 ± 1.12	21.12 ± 1.64

†Ct values ≥ 40.0 or No Ct detected

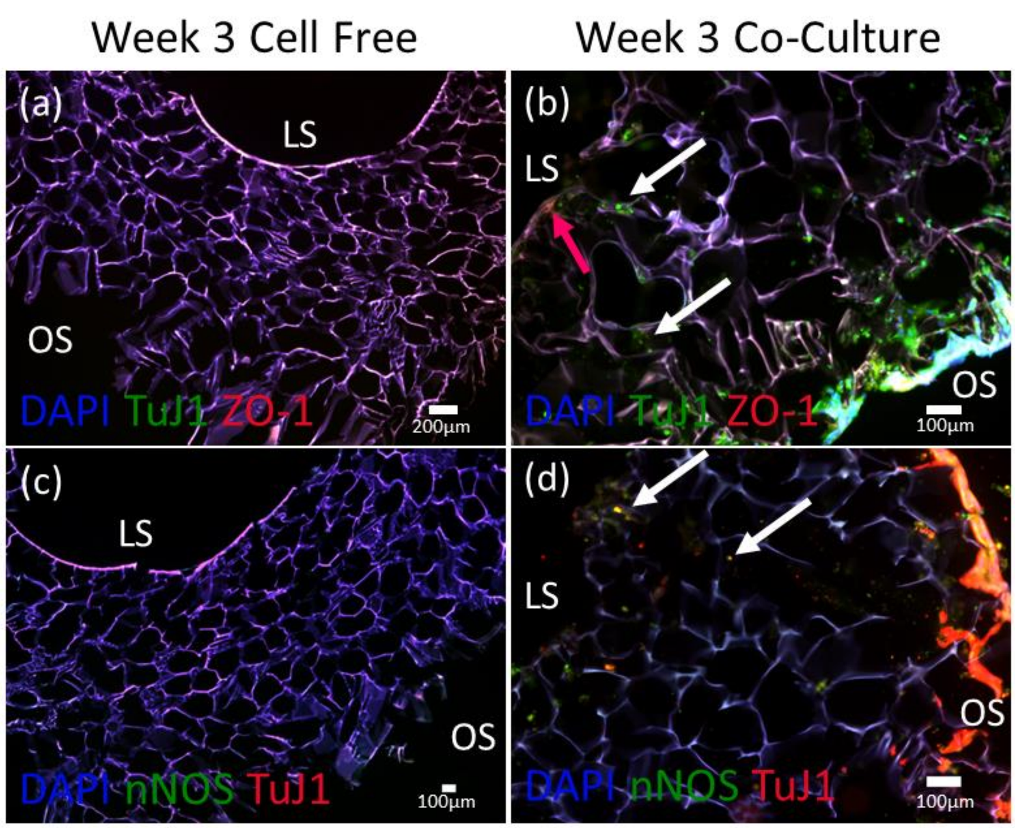

Figure 2-5: Immunostained sections of hiNSCs infiltrating toward scaffold lumen in co-cultured scaffolds. Panel a-b, pan neuronal marker beta III tubulin TUJ1 (green), tight junction marker ZO-1 (red) indicates epithelium (magenta arrow), and nuclear stain DAPI (blue) on 3D scaffold lumens at week 3. White arrows indicate clusters of neurons that have infiltrated the scaffold. Panel c-d, TuJ1 (red), neuronal NOS inhibitory neuron nNOS (green) (white arrows), and DAPI (blue) on 3D scaffold lumens at week 3.

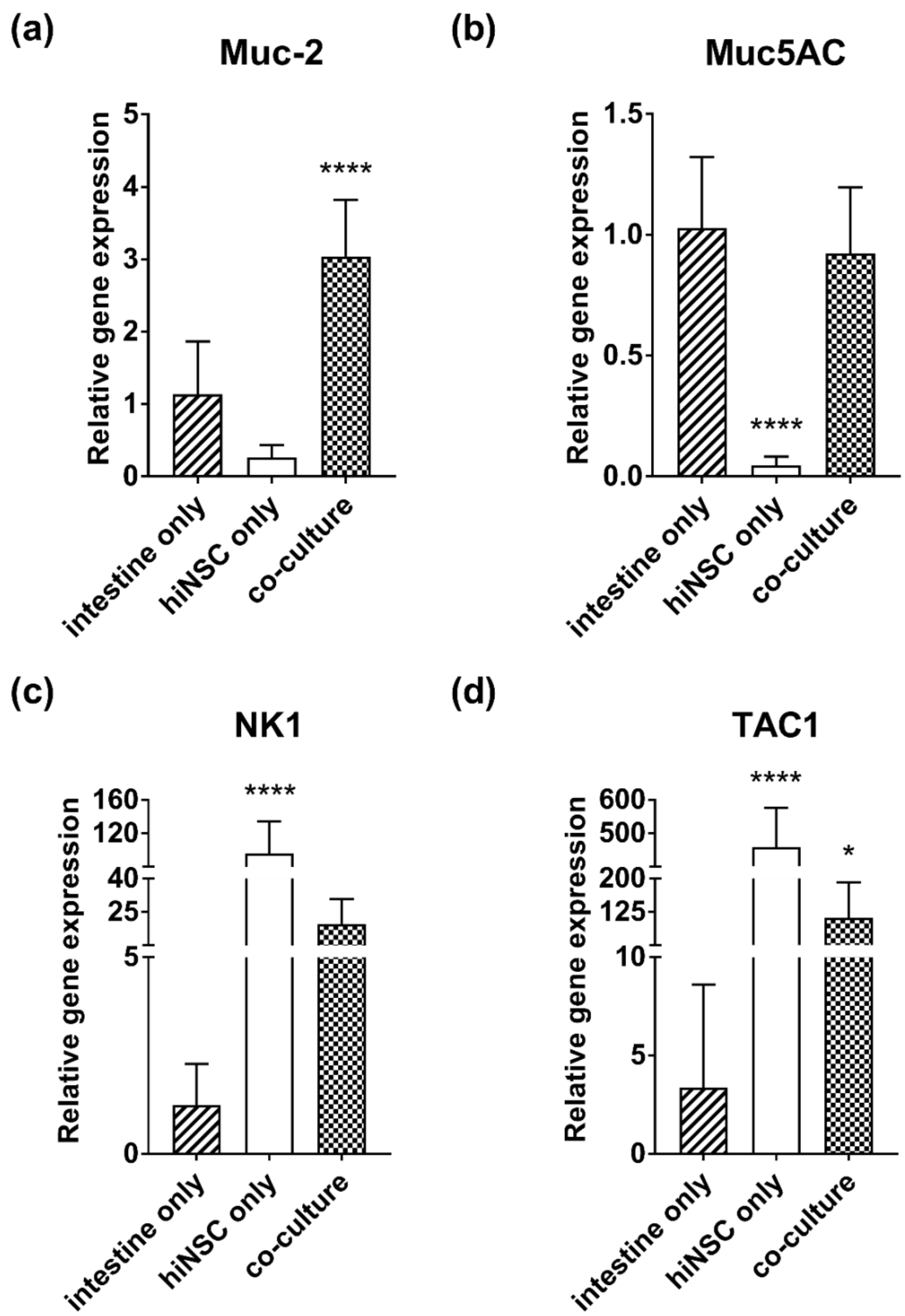

Figure 2-6: Quantitative reverse transcription-polymerase chain reaction (qRT-PCR) fold change in ivENS scaffolds as compared to intestine only scaffolds at week 5. Gene expression levels of two intestinal epithelial mucosal markers, including Muc-2 and Muc5AC, and two Substance P cascade markers, including receptor NK1 and Substance P precursor TAC1, were evaluated. The fold-change in mRNA expression was compared with intestinal only scaffolds at week 5 post hiNSC cell seeding using 18s as the housekeeping gene. * P = 0.0157 and **** P<0.0001, the mean, based on technical replicates n=9 for co-culture and intestine, n=6 for hiNSC only.

4 DISCUSSION

Our bioengineered ivENS demonstrated that 3D tissue engineered intestinal systems could harness the properties of endogenous adult human systems in a modular, compartmentalized design capable of sustainable cultivation in vitro. Established intestinal systems utilize Enterocyte-like Caco-2 and Goblet-like HT29-MTX to study interactions with the barrier cells of the intestine, including neuronal regulators [66, 67]. We utilized these cells in conjunction with intestinal myofibroblasts (IMFs) and human induced neural stem cells (hiNSCs) to recapitulate neural epithelial interplay within the ivENS, in a system that can be sustained for at least 5 weeks. While IMF and NGF were used to create an environment that support epithelial longevity and promoted neurite outgrowth, past studies have indicated cell survival within silk scaffolds out to at least 8 weeks. [68] [10]. Endogenously, the enteric nervous system is derived from a migratory cell population whose origin is the neural crest (Hao and Young 2009). These cells complete their full caudal migration by embryonic day 7.5 in chicks [69]. In human development neural crest cells complete rostrocaudal migration between weeks 4 and 7 of development [70]. Our hiNSCs have previously shown that upon injection into the neural tube, they migrate into the peripheral nervous system as well as the brain, making special note of the innervation into the limb [23]. We have shown in this work that in addition to the previous locations, hiNSCs migrate into the intestine of chick embryos prior to D12-14, making them an applicable cell source for the ivENS model as they respond to migratory cues that the endogenous population experiences (**Figure 2-2**).

Human induced neural stem cells (hiNSCs) were successfully incorporated into 3D intestinal tissue engineered scaffolds to fabricate an innervated intestinal scaffold to enable a system for the study of the enteric nervous system. Scaffolds tested in all three cell seeding conditions within the same medium maintained metabolism and cell function over time, we determined that the earliest time point at which scaffolds would be fully viable for downstream use was between 2-3 weeks of culture (**Figure 2-3**, **Figure 2-5**). To indicate the longevity of hiNSC viability within the spongy silk scaffold in SMGM: DMEM medium, live staining was performed and indicated cell survival within scaffolds past 8 weeks of culture (**Figure 2-4**). To verify neurons were infiltrating into the scaffolds, transverse cryosections of the lumen were prepared of the full area of the scaffolds. These sections showcased neural cells expressing TuJ1 in the bulk of the scaffold and toward the lumen of the scaffolds. Pockets of inhibitory nNOS+ enteric neurons were seen in the scaffolds as well (**Figure 2-5**), a population where the vast majority are developed during embryogenesis [71]. These nNOS+ neurons are highly expressed in the myenteric plexus and weakly expressed in the submucosal plexus of the enteric nervous system [72].

Maintaining barrier function within the lumen following the incorporation of the ENS component of the scaffolds is pertinent to future experimental utility of the system. Analysis of mRNA expression at 5 weeks for transcription factors implicated in barrier function explores the mucus cascade as a proof of concept mechanism for model application. For future work, this allows for scaffolds to be subjected to treatments between 2-3 weeks, when we believe infiltration spans the entirety of the scaffold bulk space, and then taken out at least 2 additional weeks while being exposed to treatment conditions. The ivENS increased or maintained the production of mucosal markers following the addition of the hiNSCs in the co-culture system at 5 weeks of culture. Muc-2 is the common mucus found in the small intestine, and Muc5AC is produced by HT29-MTX cells [73]. There was a 3-fold increase in the expression of Muc-2 in co-culture systems compared to intestinal mono-culture (INT). For Muc5AC, the expression levels were maintained in co-culture systems compared to INT systems (**Figure 2-6**, b). It should be noted that each cell type in co-culture conditions were seeded with the same cell numbers as the mono culture controls. As the same amount of mRNA was utilized to reverse transcribe the cDNA used for our qRT-PCR, 400ng, for all scaffolds, the co-cultures had lower total ratios of each cell type compared to the mono culture controls. Regardless, not only was the mucosal barrier function maintained, but there was an increase in the expression of TAC1 transcription factor upon incorporation with the hiNSCs compared to intestine only scaffolds.

The substance P cascade was explored as a potential mechanism of action for the increase in mucosal markers. Substance P (SP) is associated with inflammatory processes (specifically neurogenic), digestive motility and various gut functions, as well as pain perception and emesis. SP and other tachykinins are primarily localized in the myenteric and submucosal plexuses of the enteric nervous system, where they supply all gastrointestinal effector systems [74]. SP levels fluctuate in various human diseases, such as ulcerative colitis where patient levels average 170±46 pg/mg of tissue biopsy, and chronic severe constipation where averages are 19.9±8.2 pg/mg, compared to normal subjects at 71±18 pg/mg [75]. SP, calcitonin gene–related peptide (CGRP), and neurokinin A elicit the secretion of gastric mucus in rats in vivo [76]. Although these interactions have been studied in animal models, there is a gap in knowledge as it relates to human tissues. Through our ivENS models we have showcased an increase in both Tac1, the SP precursor, and Muc-2 transcription in the co-culture systems compared to INT systems (**Figure 2-6**, d). This suggests a correlation between the addition of hiNSCs, including a substance P positive cell population, and the 3-fold increase in the expression of Muc-2 in co-culture systems with the addition of a neuronal vs intestinal mono-culture system.

Continuous culture of these neurons in our compartmental model allows for the ability to probe discrete cell interactions, such as the substance P mucus cascade, to further elucidate the role of the ENS in various physiological mechanisms, which has multiple downstream applications for understanding the neural circuits controlling the intestine. Further, in the future, this new tissue model can be further adapted to study pathological conditions and potential treatment options for the enhancement of human intestinal health. In addition, the system can be adapted to organoid-based systems, as we have shown in our intestinal tissue systems [65], providing an even more relevant system to study the types of interactions identified in the present work.

TROUBLESHOOTING

Development of a non-invasive protocol for scaffold Substance P secretion

Substantial effort was made to develop a reliable and sensitive detection protocol for substance P secretion from ivENS scaffolds. The idea was to develop a non-invasive method to probe scaffold activity. The protocol was ultimately abandoned as the levels of Substance P detected throughout the multiple trials were close to the detection limit of the enzyme-linked immunosorbent assay (ELISA, Abcam ab133029) and our standard curve resolution was not linear at lower levels, so we could not rationalize the variability in values when comparing scaffolds.

The ability for ivENS scaffolds to secrete SP into the culture medium would provide a useful *in vitro* tissue tool for studies of changes between the epithelium and the enteric nervous system in response to treatment conditions. Our original hypothesis was that the ivENS would produce a baseline amount of SP that could be detected in the medium by ELISA. Medium samples (3ml/scaffold) were collected from scaffolds following 2 days of culture and assessed utilizing the Abcam Substance P *in vitro* competitive ELISA kit. For this method the amount of color detected is inversely proportional to the amount of SP captured from the sample. Utilizing this method levels of SP were undetectable. We hypothesized that that was due to samples producing low levels of SP, thus the concentration in the medium was too low for detection.

Samples were then prepared for concentration. Medium was collected in 50 ml conical tubes from scaffolds (3ml/scaffold) and frozen at a -80°C, samples were then lyophilized overnight. Care was made to not allow samples to thaw between transportation from the -80°C to the lyophilizer as any liquid would cause the sample to bubble and could cause potential sample loss. Once samples were lyophilized, they were reconstituted in distilled water for a final concentrated 6x solution of sample. Scaffold free medium was prepared in the same way for creation of the standard curve. On these runs the samples had detectable levels of SP (**Figure 2-7**), but they were very close to the sensitivity level of the kit. Another issue we found was occasionally the percent bound, which is inversely correlated to the level of substance P attachment, would yield results >100%. This trend is seen in the standard curve at lower levels of SP standard (**Table 2-3**). Our hypothesis is that there may be an interaction between a medium component and the ELISA kit, such that when the non-specific binding background wells are being calculated there is greater nonspecific binding that occurs compared to the samples scaffold conditions. This component may be depleted in medium with active cultures. In addition, the process of lyophilizing to concentrate samples would not only increase the potential level of substance P, it would increase all the additional medium components and secreted factors which may cause an interaction effect blocking binding to the capture antibody.

Table 2-3 Example of standard curve produced by concentrated medium doped with varying levels of SP standard.

Final Substance P concentration of standards (pg/mL)	10000	2500	625	156.25	39.06	9.76
Percent Bound (%)	17.41	30.42	69.44	99.52	124.71	123.54

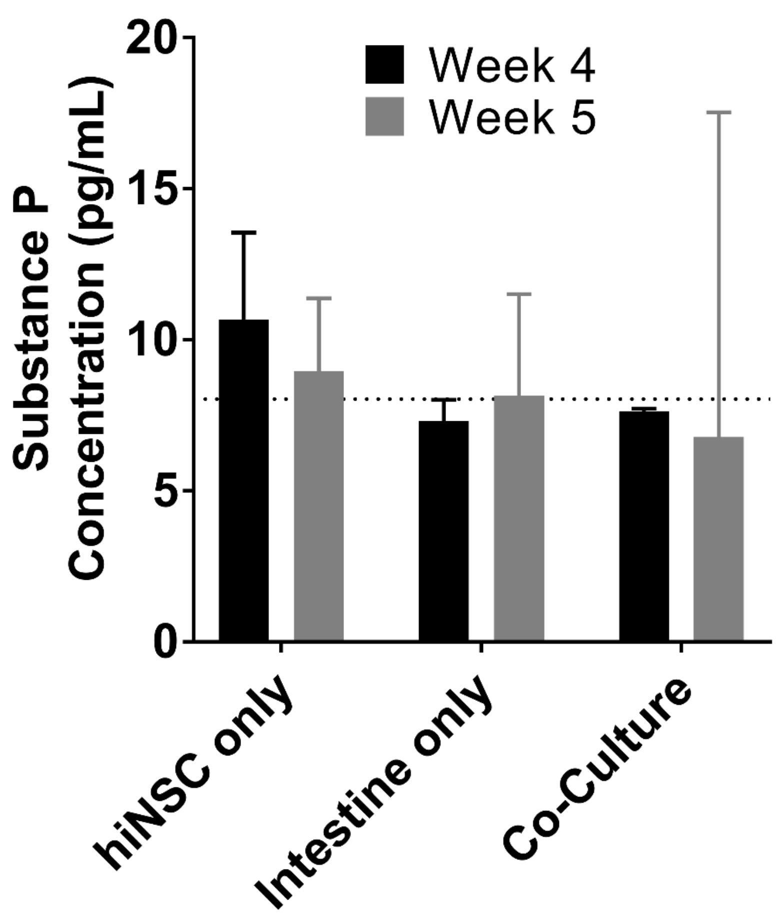

Figure 2-7: ivENS scaffold SP ELISA levels. ivENS scaffolds were grown to 5 weeks, scaffold medium samples were lyophilized and reconstituted to a 6 fold concentrated solution with distilled water. Dotted line indicates ELISA sensitivity. Samples were analyzed utilizing 2-way ANOVA, p=0.05, n=3 biological replicates, no significance detected in samples.

In order to remedy this issue of limited detection of secreted SP within the medium of each scaffold, we explored the transcription of both a precursor to SP and a receptor for SP. Expression of Tac1, which encodes for tachykinin peptide family including substance P (SP), was seen in co-culture scaffolds at week five (**Figure 2-6**, d). Neurokinin 1 (NK1), a SP receptor

This remains an area of interest, as this information would help to guide real-time analysis of future experiments with SP and other neurotransmitters, but a different strategy will need to be explored to probe scaffolds regardless of real-time accessibility (ex. WesternBlot, concentration strategies, purification strategies). In related literature SP secretion is detected in tissue or serum samples extracted from human patients, or if SP is extracted from scaffolds it seems to be best detected in systems with a majority sensory population that have been stimulated [29, 75, 77]. Minimal assays have been reported to test secretion within tissue engineered systems at baseline levels with a heterogenous cell population.

ACKNOWLEDGMENTS

This work was supported by the NIH (U19AI131126, P41EB002520, R21AI128093, R21AI128342-01, S10 OD021624). We also thank the Gates Foundation for support of these studies. EM was supported by the DoD through the NDSEG

Fellowship Program. We would like to thank Dr. Yu-Ting Dingle for assistance with Adobe Illustrator.

CHAPTER 3 : EFFECT OF MICROBIAL METABOLITES ON *IN VITRO* ENTERIC NERVOUS SYSTEM TISSUE MODEL

Adapted from manuscript authored by Eleana Manousiouthakis, Nicholas Alden, Michael J. Dente, Olivia Hofheinz, Rani Menon, Evelyn Callaway, Clint Cheng, Arul Jayaraman, Kyongbum Lee, and David L. Kaplan [78].

Contributions: EM and NA are co-first authors of this work. EM, NA, KL, and DK designed and conceived the study. EM, NA, MD, OH, RM, EC, and CC conducted the experiments and acquired the data. EM, NA, and MD contributed to analysis and interpretation of the data.

ABSTRACT

Over the past decade the role of the human gut microbiome has been linked to both intestine and brain maladies. Although correlations have been drawn between changes in microbial populations and disease states, it is unknown how these correlations are caused or what mechanisms may be at play. *In vitro* tissue models of the enteric nervous system offer an adaptable platform to study specific cell responses to microbial influence. In this work we explored the effect of microbial metabolites utilizing our engineered *in vitro* Enteric Nervous System model (ivENS) consisting of enterocyte-like (Caco-2) and goblet-like (HT29-MTX) cells to form the intestinal epithelial layer, intestinal myofibroblasts (IMF) to simulate the stromal layer, and human induced neural stem cells (hiNSCs)

differentiated into enteric nervous system neural cell types to emulate the enteric nervous system. Our studies utilize Taurine and Kynurenate, metabolites associated with the gut microbiome, and lipopolysaccharides (LPS) from *E. coli* as a positive control, to determine the inflammatory response of the enteric nervous system associated with the microbiome.

In the work described below we indicated that microbial metabolite and LPS treatment levels utilized have no immediate effect on scaffold viability via alamar blue seen over the course of 12 days, thus there is no treatment dependent detriment to the scaffold viability. The cytokine response of ivENS systems to purified microbial metabolites showed levels of IL-8 and IL-6 with no treatment specific changes, and levels of MCP-1 were altered depending on treatment group and had a sharp increase in production in LPS positive control scaffolds. When samples were inoculated with Taurine or Kynurenate 24h hours prior to treatment with LPS. LPS treated samples showed a marked increase in MCP-1 levels, but the scaffolds that were pretreated with microbial metabolites did not see the same increase at the 24 hour mark post LPS treatment. Scaffolds that received metabolite pretreatment showed similar levels of MCP-1 as untreated control scaffolds, indicating that these metabolites contribute a protective effect against mounting a pro-inflammatory signaling in response to LPS treatment. These results showcase the potential for utilizing specific microbial communities and their metabolites to promote anti-inflammatory effects in patients.

1 INTRODUCTION

The exact mechanisms with which the gut communicates with the central nervous system are unknown. Due to this, the role of enteric flora in immune-response within the enteric nervous system (ENS) in patients with brain and gut disorders remains unidentified [3]. Advances in the fields of microbial phenotyping have allowed for massive undertakings such as the NIH Human Microbiome Project to characterize the human microbiome and identify any links between disease states and the diversity of the commensal microbiome [79, 80].

Specific members of the microbiome have been implicated in stimulating cellular signaling in the gut epithelia [80]. Furthermore, animal studies have shown changes in adult germ-free (GM) mice compared to specific pathogen free (SPF) mice, such as significant changes in anxiety-like behavior utilizing elevated plus maze (EPM) experiments [81, 82]. There are also demonstrated cases of interactions between microbial derived metabolites and host signaling pathways [83]. As such, the metabolome of the microbial community within the gastrointestinal tract (GI) is of particular interest to human health and should be studied further.

The commensal relationship of microbial communities with their mammalian hosts is thought to remain possible, as long as host cells remain tolerant to the immune stimulation that is generated by these microbial communities. Phylum-wide studies have indicated that there are microbiome-derived mechanisms that actively promote host immune tolerance to the gut microbiota [84]. Pro-inflammatory stimulants of both Toll-like receptors TLR2 and TLR4 are produced by the endogenous microbiota, these receptors can be triggered by lipopolysaccharides (LPS) derived from *E. coli* [85]. Some bacteria within the commensal population, such as *Bacteroides dorei*, produce an immunoinhibitory form of LPS that can silence the TLR4 signaling. Despite research within the field these immune mechanisms have yet to be fully elucidated, and the metabolome may play an important role in regulation which requires further study in both human *in vitro* models and representative animal models.

In order the elucidate the role of microbial metabolites that alter host physiology in the intestine, metabolites that differ due to alterations in the gut environment must be studied. Previous work has identified some metabolites of interest such as taurine (T) and kynurenate (K), that are known to contribute to perturbations in gut health [46, 86, 87]. While gut microbiota–to–brain signaling systems have been extensively studied in animal models, human systems are understudied [3]. Thus, human *in vitro* innervated intestinal tissue models would significantly improve our ability to explore the effects of microbial metabolites at the epithelial level and on the ENS.

2 METHODS

2.1 Scaffold generation for co-cultured ivENS

In vitro ENS (ivENS) co-cultured tissues were prepared as per our previous protocols in Chapter 2; in brief $4x10^5$ epithelial cells were seeded in the lumen of the scaffold at a 3:1 ratio of Caco2:HT29-MTX, and $3x10^5$ intestinal myofibroblast cells were seeded in the bulk of the scaffold on day 0 (D0). On D0, hiNSCs were transferred from colonies to gelatin coated plates, and fibroblast growth factor (FGF) was removed from the medium to allow for differentiation to neural lineage [23, 47]. On day 7 (D7) following maturation of the intestinal components within the scaffold, $1x10^6$ hiNSCs were seeded on the perimeter of the scaffolds and guided into the bulk with 50ng/mL neural growth factor (NGF) supplemented into the medium in addition to supplementation into the collage used to fill the silk scaffold pores at D0.

2.2 Cell culture

2.2.1 Cell sources: The human intestinal epithelial cells, Caco2 were obtained from ATCC (Rockville, MD), and HT29-MTX from the Public Health England Culture Collection (Salisbury, Great Britain). These were cultured in DMEM supplemented with 10% fetal bovine serum, 10 μg/mL human transferrin (Gibco, Gaithersburg, MD). Human Intestinal Myofibroblasts (IMF) (Lonza, Portsmouth, NH) were cultured in SmGM™ Bullet Kit. For Caco-2 and HT29-MTX, cells from passage number 38–50 were used for cultures, and for IMF, passage number 3–5 were used.

Human induced neural stem cells (hiNSCs) were generated as previously described [23] and cell line #5 was donated by Dr. Dana Cairns for use in these studies. Cells were grown on mouse embryonic fibroblast cells (MEF) (ATCC, Rockville, MD) feeder layers that had been inactivated by mitomycin C. hiNSCs were enzymatically passaged as colonies using trypsin-like enzyme, TrypLE (Invitrogen), expanded, and cultured until sub-confluent (80-90%) before the next passaging. Colonies were cultured in KO medium (knockout (KO) DMEM supplemented with 20% KO xeno-free SR, 20 ng/mL recombinant bFGF, 1% Glutamax, 1% antibiotic-antimycotic, and 0.1 mM β-mercaptoethanol) [23]. Cell used for seeding were differentiation toward neural phenotype by transferring hiNSCs from colonies onto gelatin coated plates and removing the fibroblast growth factor from the KO medium for 7 days of culture, at which point cells were detached using TrypLE and added to the scaffolds as described in the seeding protocol in Chapter 2. All cells were maintained in a humidified chamber at 37°C with 6% CO_2 prior to incorporation into scaffolds.

2.2.2 Mycoplasma testing: All generated lines used for these experiments tested negative for mycoplasma contamination using PCR based Mycoplasma Testing services from Charles River. In brief, 3 undiluted 200 µL samples of each cell culture were collected following detachment from culture plates (Trypsin-EDTA, or TrypLE for the hiNSCs) and resuspended in respective standard culture medium. Samples were frozen at -80°C and shipped overnight on dry ice. During culture of ivENS, all medium was supplemented with 0.2% primocin (Invivogen, San Diego, CA) to prevent future contamination of long-term scaffolds.

2.3 Metabolite and lipopolysaccharide preparation

Metabolites taurine (T) and kynurenate (K) were dosed at 10µM, 1mM stock solutions (100x) of T and K were prepared in water for injection (WFI). Untreated medium was supplemented with WFI at the same volume as that used for the metabolite conditions. For example, when preparing 250 mL of medium, 2.5mL of WFI with or without metabolite was added to 247.5 mL of medium (1:1 ratio of 1xDMEM and SmGM, supplemented with 50ng/mL of NGF and 0.2% primocin). For conditions with Lipopolysaccharides (LPS) from e.coli, scaffolds were dosed at 5µg/mL of LPS added at the time of treatment to premade medium (with or without metabolites) and filter sterilized.

2.4 Treatment of metabolites

2.4.1 Effect of microbial metabolites on ivENS

Initial metabolites of interest, Taurine (T) and Kynurenate (K) were determined via work from the Jayaraman and Lee labs. In brief, antibiotic-induced dysbiosis was triggered at 9 weeks of age in female wild-type C57BL/6T mice (Taconic Biosciences, Albany, NY) utilizing an antibiotic cocktail of 225mg ceftazidime, 108mg bacitracin, 108mg neomycin, 43.2mg ampicillin, 21.6mg meropenem, and 6.48mg vancomycin dissolved in 4.5mL autoclaved water. Brain tissue, feces, serum, and cecal content was collected for untargeted LC-MS. Samples were reconstituted in a solution of methanol/water (50% v/v). Profiling of sample metabolites was performed using the methods and equipment described previously [88]. This method determined changes in both Taurine and Kynurenate presence dependent sof dysbiosis condition.

Co-cultured ivENS were grown to 2 weeks of culture (N14/M0) and treated with either metabolites T and K, LPS positive control, of untreated medium (**Figure 3-1**). Medium with LPS was dosed for 24 hours and then replaced with untreated medium for the duration of testing out to 12 days of culture under treatment conditions (M12).

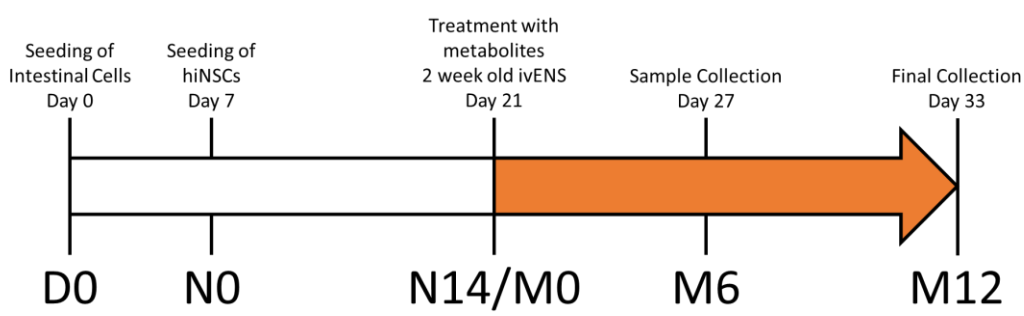

Figure 3-1: Experimental timeline for metabolite treatment.

2.4.2 Protective effects of microbial metabolites on ivENS

For protective effects experiments, samples were prepared in similar conditions up until metabolite treatment (N14/M0). Scaffolds were pretreated with or without medium doped with metabolites (T or K) 24 hours prior to a 24 hour with or without LPS exposure. **Table 3-1** indicates the various treatment conditions that the ivENS were exposed to during the duration of the experiment.

Metabolite addition was supplemented in the medium throughout the experiment (M0-M12) and LPS treatment was only received for 24 hours on M1, 24 hours following metabolite inoculation.

Table 3-1: Table of treatment conditions for microbial protections experiments. *1 cell free scaffold added for each condition, ** control for +LPS conditions

Condition*	**1**	**2**	**3**	**4**	**5**	**6**
Compound 1 (Taurine)	-	-	-	-	+	+
Compound 2 (Kynurenate)	-	-	+	+	-	-
LPS	-	+	-	+	-	+
# Replicates	3	3	2**	3	2**	3

2.5 Alamar Blue Assay

Alamar blue was used to measure the metabolic activity of each of the scaffold conditions to ensure that treatment conditions had no effect on metabolic activity between scaffold conditions. A 10% alamar blue solution was made in a one to one ratio of SmGM and DMEM medium and incubated with the samples for 3 hours at 37°C. Following incubation, samples were read on a plate reader in triplicate and scaffolds were rinsed 3 times in PBS prior to having their respective medium condition replaced.

2.6 Cytokine expression

Samples were collected from scaffold medium prior to medium exchanges (500µL/scaffold), flash frozen in liquid nitrogen, and stored at -80°C until analysis. Sample were assessed using LEGENDplex™ Human Inflammation Panel 13-plex (BioLegend, 740118) was run on an Attune NxT Flow Cytometer with Autosampler for sample loading directly from V-bottom 96 well plates. Parameters for gating were set following LEGENDplex protocol for Beads 3. All samples were diluted 3-fold and run with their respective cell free controls to normalize for background detection following analysis.

LEGENDplex v8.0 proprietary Data Analysis software was utilized to correlate Attune NxT flow data to cytokine levels. Bead size A was affiliated with 6 cytokines (IL-6, MCP-1, TNF-α, IFN-γ, IFN-α2, IL-1β), while bead size B was affiliated with 7 cytokines (IL-33, IL-23, 1L-18, IL-17A, IL-12p70, IL-10, IL-8). Following analysis all samples were baseline corrected in GraphPad Prism to remove respective cell-free (CF) scaffold reading for each sample.

2.7 Statistics

Two-Way ANOVA with Tukey test was applied in the comparison between multiple experimental groups. All data are expressed as mean ± standard deviation. A p-value less than 0.05 was used to determine significance. One-Way ANOVA with Tukey test was applied to MCP-1 data within each time point. All data are expressed at fold change mean ± standard deviation. A p-value less than

0.05 was used to determine significance. All statistical analysis was carried out using GraphPad Prism 7 software (GraphPad Software, CA, USA).

3 RESULTS

3.1 Scaffold viability following metabolite treatment

Cultures were assessed for metabolic activity following co-culture of hiNSCs (N0) until day 12 of metabolite culture (M12) (Figure 3-1). Conditions include treatment with metabolites associated with the microbiome, taurine and kynurenate, and pro- inflammation control utilizing lipopolysaccharides (LPS) from *E. coli*. Cultures of ivENS maintained metabolic activity (Figure 3-2) throughout the experiment duration, no significant difference was seen between groups within each time point. Values were similar to levels of florescence intensity (RFU) seen in previous experiments with treatment free co-culture scaffolds at similar time points (Figure 2-3). No significant interaction effect was present between time and RFU measurements.

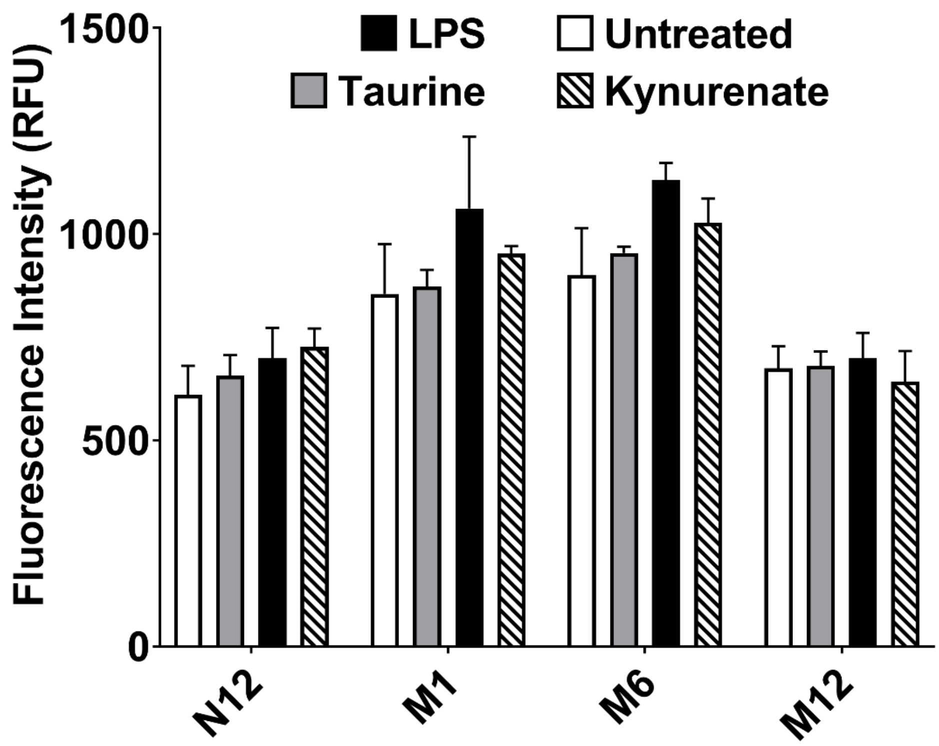

Figure 3-2: Alamar Blue ivENS scaffolds after 12 days of culture pretreatment (N12) and post metabolite treatment (24h, M1; 6 days, M6; 12 days, M12). Scaffold metabolic activity was assessed over 4 weeks total, with no statistical difference between treatment groups within each time point. The mean ± standard deviation of fluorescence, based on 3 independent biological replicates.

3.2 Cytokine activity within ivENS

Within the 13-plex kit, some cytokines were consistently undetectable (Table 3-2). MCP-1, IL-6, and IL-8 showed consistent detection across experimental treatments. Production of MCP-1 was altered depending on treatment group (Figure 3-3). While IL-6 and IL-8 were present in the medium, neither cytokine showed any significant changes with treatment (Figure 3-4, Figure 3-5).

Table 3-2: Cytokine detection within ivENS. n.d. denotes levels that were not detected, cytokines with the label, On Occasion, were not decetable on some runs and thus not reliably present in systems. Values presented are the raw value from the LEGENDplex analysis software showcasing the range present from 3 separate experimental runs.

Cytokine	Detection	Level
IL-1β	No	n.d.
IFN-α2	No	n.d.
IFN-γ	No	n.d.
TNF-α	No	n.d.
MCP-1	Yes	<1.2-15,000 pg/mL
IL-6	Yes	<2.41-230 pg/mL
IL-8	Yes	n.d. – 22482 pg/mL
IL-10	No	n.d.
IL-12p70	No	n.d.
IL-17A	No	n.d.
1L-18	No	n.d.
IL-23	On Occasion	n.d. – 198 pg/mL
IL-33	On Occasion	n.d. – 728 pg/mL

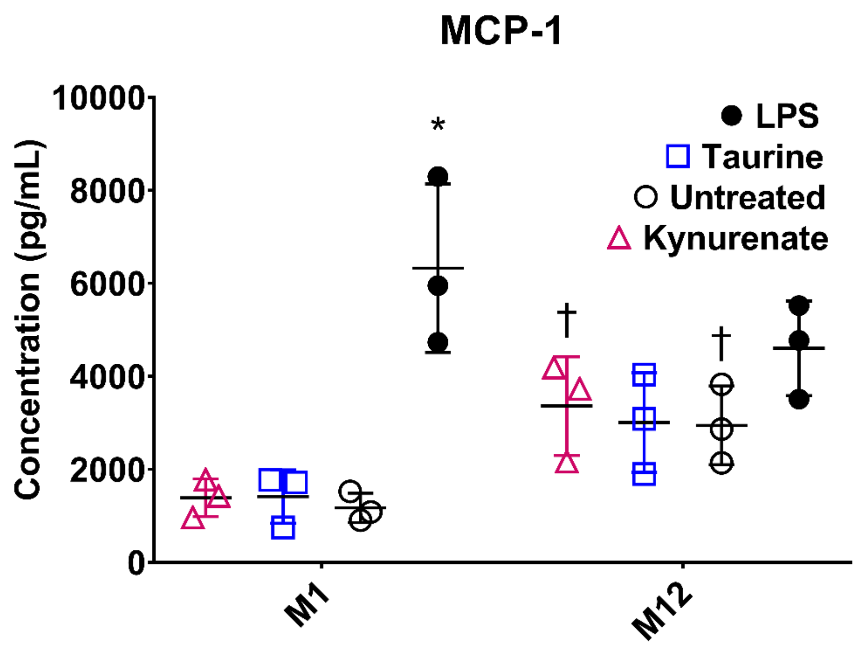

Figure 3-3: MCP-1 levels at 24h (M1) and 12 days following treatment (M12). *p<0.0005, compared within dates. † p<0.05, compared between dates. 2 Way ANOVA performed. The mean ± standard deviation of concentration, based on 3 independent biological replicates.

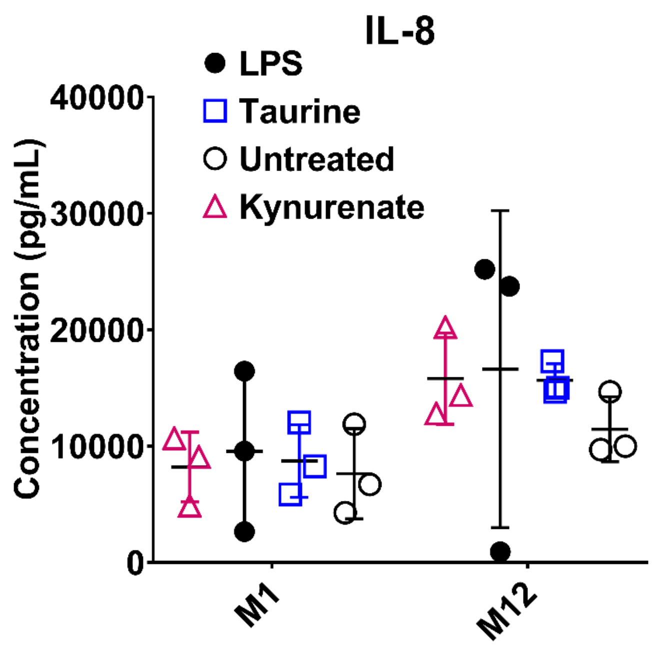

Figure 3-4: IL-8 levels at 24h (M1) and 12 days following treatment (M12). *p<0.0005, compared within dates. † p<0.05, compared between dates. 2 Way ANOVA performed. No significance was detected. The mean ± standard deviation of concentration, based on 3 independent biological replicates.

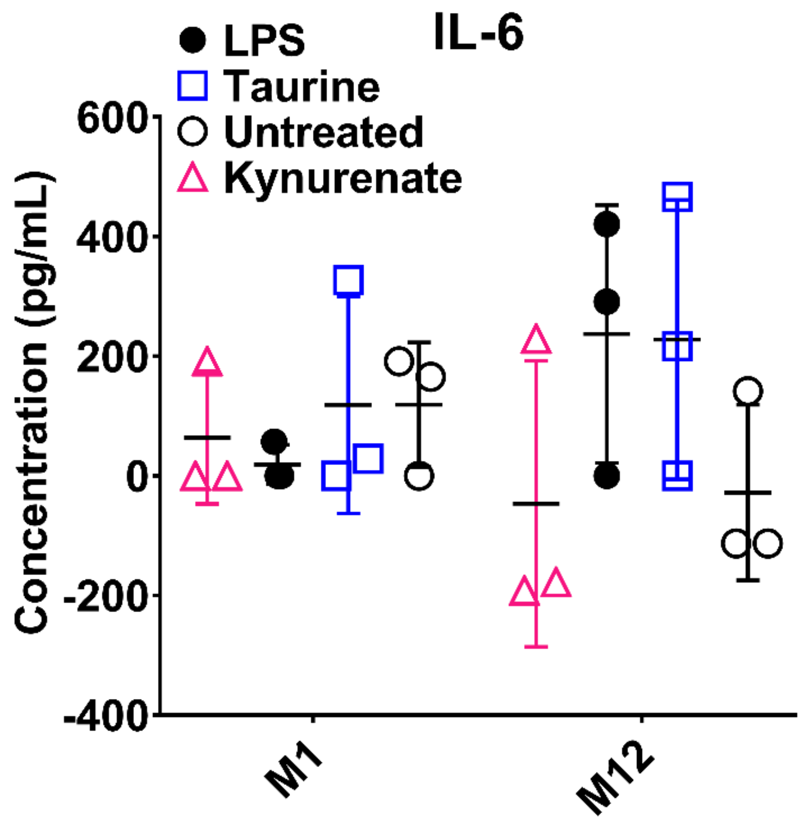

Figure 3-5: IL-6 levels at 24h (M1) and 12 days following treatment (M12). *p<0.0005, compared within dates. † p<0.05, compared between dates. 2 Way ANOVA performed. No significance was detected. The mean ± standard deviation of concentration, based on 3 independent biological replicates.

3.3 Microbial protection in ivENS

For assessment of microbial metabolite protection, we focused on MCP-1 production. No significant differences were seen at 1 hour following LPS treatment (**Figure 3-6**). LPS treatment caused a significant increase in MCP-1 production, which diminished following pre-treatment with either T or K at 24 hours of LPS treatment (Figure 3-7).

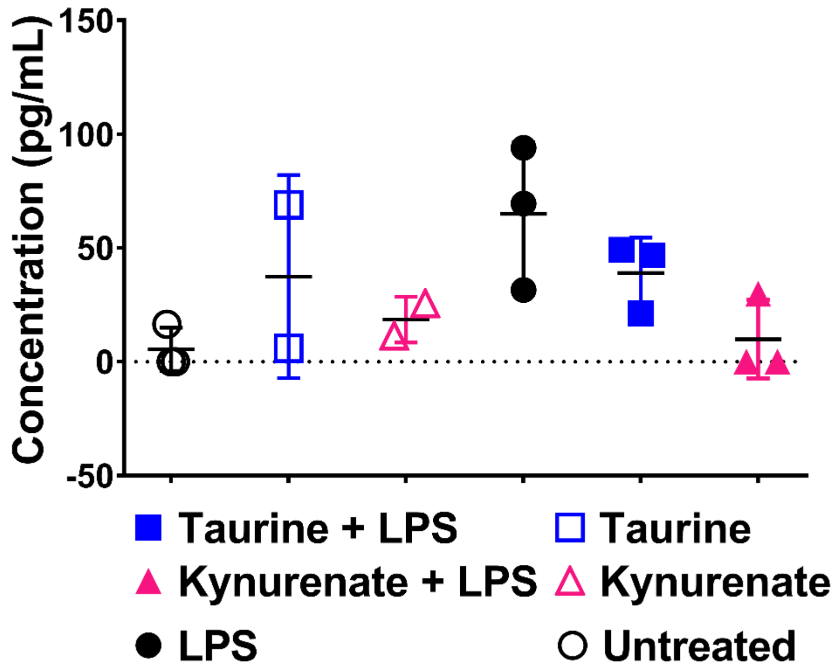

Figure 3-6: MCP-1 levels 1h following LPS+ or LPS- treatment. Scaffolds treated with metabolite+ (taurine or kynurenate) or metabolite- medium 24h prior to LPS+ or LPS- exposure for an additional 24h. 1 Way ANOVA performed, no significance determined. The mean ± standard deviation of concentration, based on 3 or 2 independent biological replicates.

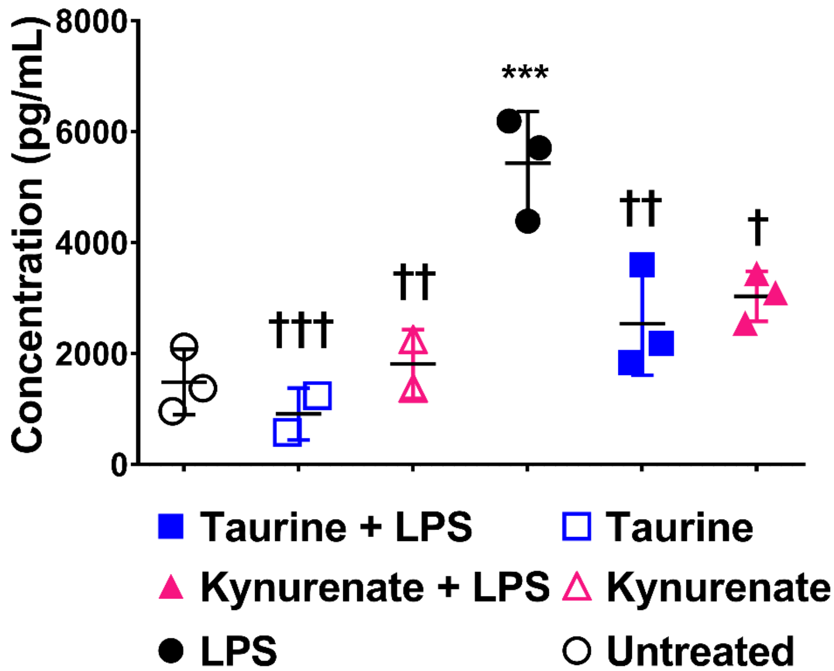

Figure 3-7: MCP-1 levels 24h following LPS+ or LPS- treatment. Scaffolds treated with metabolite+ (taurine or kynurenate) or metabolite- medium 24h prior to LPS+ or LPS- exposure for an additional 24h. *$p<0.05$, compared to untreated. † $p<0.05$, compared to LPS. 1 Way ANOVA performed. The mean ± standard deviation of concentration, based on 3 or 2 independent biological replicates.

4 DISCUSSION

Various microbial metabolites are in contact with the length of the gastrointestinal tract and provide an interesting target to perturb tissue engineered enteric nervous system models at the epithelial level. Microbiota deficiency causes alterations of an assortment of metabolites, including the circulating availability of kynurenine [86]. Microbiota-modulated metabolites, including taurine, have been implicated in changes to innate immunity [89].

Human *in vitro* innervated intestinal tissue models allow us to explore the effects of microbial metabolites at the epithelial level and on the ENS. In order to explore the effect of these individual microbial metabolites and the inflammatory response affiliated with them, ivENS scaffolds are subjected to treatments with purified microbial metabolites taurine (T) and kynurenate (K), as well as pro-inflammation control of lipopolysaccharides (LPS) from *E. coli*.

Tissue viability is pertinent to continuation of in vitro experiments involving the effects of microbial metabolite. We hypothesized that the dose levels chosen would have no immediate effect on scaffold viability. Alamar blue data shows each scaffold condition causes no significant difference in metabolism within the scaffolds Figure 3-2. Given this, there is no treatment dependent detriment to the scaffold viability and these dosages can be utilized to probe the cellular effect of microbial metabolites.

The microbiota has been implicated in host immune response and alterations in cytokine production [89, 90]. The cytokine response of ivENS systems to purified microbial metabolites was determined using a 13-plex kit, but the majority were undetectable (**Table 3-2**) aside from MCP-1, IL-6, and IL-8. Levels of IL-8 and IL-6 show no treatment specific changes, but MCP-1 altered depending on treatment group and had a sharp increase in production in LPS positive control scaffolds (Figure 3-3, **Figure 3-4**, **Figure 3-5**). Cytokine monocyte chemoattractant protein-1 (MCP-1) secretion in response to LPS treatment is linked to Toll-like receptor (TLR) expressed by neurons in the enteric plexuses of rats [91]. This could be a potential mechanism of action within the ivENS tissue systems and will be further explored in future studies as TLR4 is associated with the intestinal epithelium and knockout TLR2 enteric neurons exhibit smaller ganglia [92, 93].

The capability of MCP-1 production in ivENS allows for the exploration of the effect of microbial metabolites on the inflammatory response in relation to the human enteric nervous system. In untreated and kynurenate treated samples, there was an increase in MCP-1 between M1 and M12. This trend is not seen in taurine treated scaffolds. Microbial metabolites have been implicated in anti-inflammatory signaling within the intestine [87], this anti-inflammatory effect may be the case with Taurine treated ivENS.

To test the protective capabilities of these microbial metabolites, samples were inoculated with Taurine or Kynurenate 24h hours prior to treatment with LPS. At 1 hour following LPS treatment no differences were detected in MCP-1 levels (Figure 3-6). At the 24 hour mark, LPS treated samples showed a marked increase in MCP-1 levels, but the scaffolds that were pretreated with microbial metabolites did not see the same increase (Figure 3-7). Scaffolds that received metabolite pretreatment showed no significance when compared to untreated control scaffolds. This shows that metabolites associated with the microbiome contribute a protective effect against mounting a pro-inflammatory signaling in response to

LPS treatment. These results indicated the potential for utilizing specific microbial communities to promote anti-inflammatory effects.

TROUBLESHOOTING

Substantial effort was made to develop a metabolomics protocol to detect medium changes in scaffold metabolites based on treatment conditions. Untargeted analysis following previous methods was performed [88], but low or no detection of components outside of medium depletion were indicated within scaffold systems. Samples were concentrated using extraction methods for LC/MS, and detection was mostly depleted nutrients. Given this, we halted attempts to assess secreted metabolites and instead focused our efforts on intercellular metabolites. Past studies allow for cell to be batch-fed such that metabolites can accumulate over 7-10 days of Chinese hamster ovary (CHO) cells in culture [88]. As the current design of our systems must be fed at least every 2 days, we were unable to build up metabolites within the cultures to the same extent as past batch-fed work where pertinent nutrients were supplemented into spent medium.

Another avenue that we explored briefly was an attempt to collect intracellular metabolites, but stacking the metabolites extraction in series with RNA, DNA, and Protein extraction from scaffolds. We were able to find one source in which this was previously done and adapted it to be utilized with our Qiagen All-Prep Kit (Qiagen, 80004) [94]. We followed the All-Prep protocol to isolate RNA and DNA.

Utilizing the flow through we attempted to perform a methanol chloroform extraction to collect both polar (methanol) and non-polar (chloroform) metabolites. We were unable to see an interphase where we hypothesized our protein would remain but attempted to continue the LC/MS sample preparation. Following sample prep our samples ended up forming a viscous solution that was unable to be utilized with our standard LC/MS protocol.

We remain interested in attempting to find a non-sacrificial solution to probe low levels of ivENS metabolites as well as neurotransmitters. We believe that in future studies, alterations in the density of hiNSCs seeded within the scaffolds to increase the total neuron count at the time of medium collection may allow for a higher level of neuron related metabolites to be secreted and detected within the medium. Untargeted methods are still being explored as a means to assess the response of ivENS to treatment conditions.

ACKNOWLEDGMENTS

We would like to thank Dr. James Van Deventer and Jessica Stieglitz for allowing us access to run our samples on the Attune NxT and for guidance during our initial assay set up. This work was supported by the NIH (U19AI131126, P41EB002520, R21AI128093, R21AI128342-01, S10 OD021624). We also thank the Gates Foundation for support of these studies. EM was supported by the DoD through the NDSEG Fellowship Program.

CHAPTER 4 : FUTURE DIRECTIONS

We have developed an *in vitro* enteric nervous system (ivENS) tissue model that utilizes human derived cells, is capable of long-term culture, and mimics endogenous ENS function to form an adaptable model suitable for biological, therapeutic, and regenerative applications. This technology opens the door for researchers to utilize a simple, yet robust model system to study questions surrounding the gut-brain axis. Additionally, this tissue model creates a hospitable system to study microbial interactions and communication with the ENS of the intestine.

The enteric nervous system is home to a variety of neurons, with at least 14 enteric neuron subtypes present [95]. Future work would proceed to ensure differentiation of hiNSCs into varied enteric nervous system cell types, such as ascending interneurons and descending interneurons, and characterize their functional properties within the model. Each of the neurons plays a different role within the ENS and to develop a fully functional ENS model all roles must be explored.

In addition to the roles of the ENS neurons, other cell types present within the gastrointestinal tract should be merged within the in vitro model. Incorporation of smooth muscle layers, regenerative crypts, patient specific cell populations, or microbial communities will bring the model closer to mimicking construction of native tissue.

1 ORGANOID ENTERIC NERVOUS SYSTEM

1.1 Background and significance

Incorporation of further heterogeneity of the epithelium within the ivENS system will further recapitulate endogenous communities, including paneth and enteroendocrine cells [96]. Organoids have been utilized in the past to form monolayers with great success, and have been shown to be seeded in a monolayer on 3D porous silk scaffolds for culture out to around 11 days of culture [65]. Our past work has indicated that hiNSCs can survive in scaffolds out to 60 days and have been co-cultures with both goblet-like and enterocyte-like cells long-term [47].

Intestinal organoids offer the capability to incorporate more epithelial diversity into the lumen of tissue models of the enteric nervous system. Within the endogenous epithelial layer, some enteroendocrine (EE) cells act as signal transducers that convert bacterial stimuli into neuronal responses [7]. A subset of EE cells, called enterochromaffin (EC) cells, are responsible for the synthesis, storage, and release of serotonin (5-HT) and present in both colonic and small intestinal organoids [97]. Animal models with 5-HT knockout have fewer paneth cells which are known to secret antimicrobial peptides like defensins [98, 99]. In addition, mucus production and microvilli polarization are key components of intestinal barrier function and organoids have the capability to produce them [65]. The addition of organoid derived epithelium would allow for the presence of paneth cells, various enteroendocrine cell populations, and goblet cells that are known to interact with the enteric nervous system and will allow for further diversity within the ivENS [100].

1.2 Methods

1.2.1 3D culture of organoid based ivENS

Organoid cultures can be expanded from an assortment of tissue regions, including ilium, jejunum, duodenum, and colon. To culture our organoids will we adapt our previous protocol to first be utilized with colon specific organoids, colonoids [65]. The bulk of spongy silk scaffolds, with 2mm diameter lumens, will be filled with collagen solution with neural growth factor 50 ng/mL (NGF, R&D Systems, Minneapolis, MN), 80% rat-tail collagen (2.05mg/mL in 0.6% Acetic Acid, First Link, UK), 10% 10X DMEM, and 10% 1X DMEM. Colonoids will be dissociated from matrigel droplets and seeded in monolayer on lumen of scaffolds. Scaffolds will be grown in growth medium for 3 days to allow colonoid derived cells to coat the luminal service before being transferred to differentiation medium.

Colonies of hiNSCs will be removed from MEF plates using TrypLE™ Select Enzyme (1X) (ThermoFisher, Waltham, MA) and pasted through a 40µm cell strainer. Strained hiNSCs will be suspended in collagen solution, 80% rat tail collagen (2.05mg/mL in 0.6% Acetic Acid, First Link, UK), 10% 10X DMEM, and 10% 1X DMEM, without NGF and coated on the peripheral edge of the mature scaffolds. The four conditions studied will include: (a) colonoid derived cells only, (b) hiNSCs only, (c) co-culture (all listed cell types), and (d) cell free scaffolds. All scaffolds will be cultured in differentiation medium, supplemented with 50ng/mL of NGF and 0.2% primocin (Invivogen, San Diego, CA).

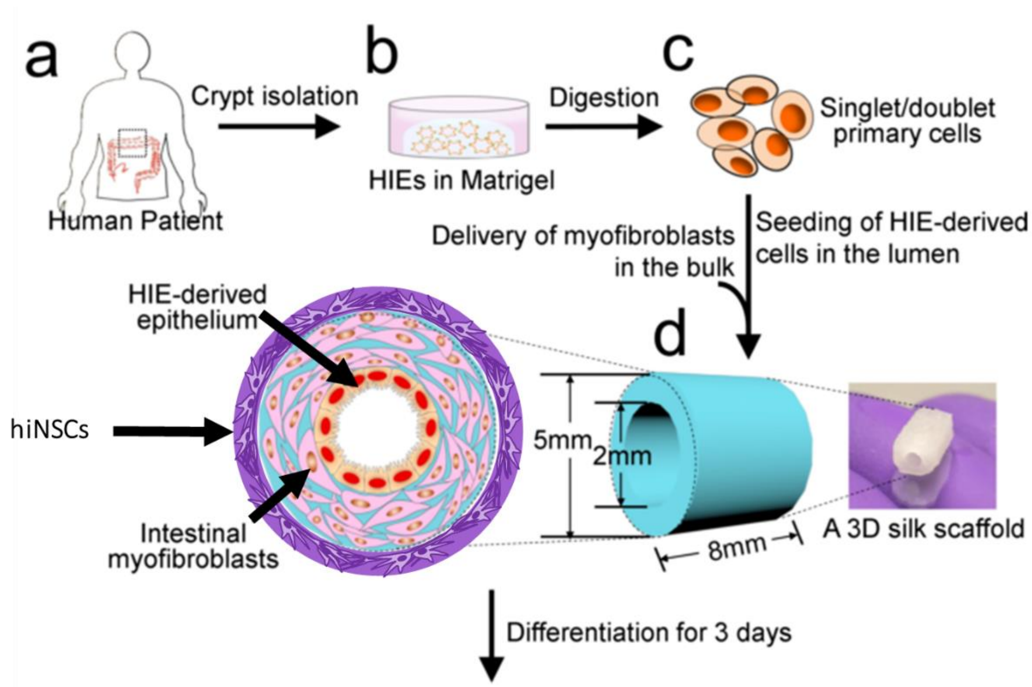

Figure 4-1: Figure adapted from Chen et al. 2017 [65]. (a, b) HIEs isolated from human patients are cultured in the Matrigel. (c) HIEs are enzymatically digested to obtain Singlet/doublet cells. (d) HIE-derived cells are seeded onto the luminal surface of a 3D tubular silk scaffold, while H-InMyoFibs are delivered into the spongy silk scaffold bulk. The purple outer ring indicates proposed seeding location of human induced neural stem cells within an organoid derived 3D spongy silk scaffold (d). The constructs are then cultured in differentiation medium for at least 3 days to induce intestinal epithelial differentiation prior to functional analysis.

1.2.2 2D preliminary compatibility tests

Human induced neural cells (hiNSCs) were cultured as described in Chapter 2. When colonoids were confluent we tested 3 seeding conditions for incorporation of hiNSCs (Table 4-1). Neurons were either seeded straight from colonies or after 1 week of differentiation in KO medium without FGF. Upon combination of neurons with colonoid cultures, co-culture systems will be maintained in differentiation medium for 5 days of culture.

Table 4-1: hiNSC and colonoid seeding conditions.

Condition	**1**	**2**	**3**	**4**	**5**	**6**	**7**
hiNSCs undifferentiated 25k (N_U)	+	-	-	-	+	-	-
hiNSCs differentiated 50k (N_D)	-	+	-	-	-	+	-
hiNSCs differentiated 100k (N_D)	-	-	+	-	-	-	+
Colonoids (C)	-	-	-	+	+	+	+
# Replicates	2	2	2	3	3	3	3

1.2.3 Epithelial cell screening via Quantitative RT-PCR

Quantitative RT-PCR will be performed to quantify the expression of Chromogranin A, for enteroendocrine cells, 5-HT, for enterochromaffin cells, and Muc-2, for goblet cells in mono-culture and co-culture silk scaffolds. Scaffold regions will be separated utilizing trypsin 0.25% to detach colonoid derived cells from the luminal surface in order to isolate epithelial cells from the neuronal cells within the bulk. Isolation will allow for the biological markers within these regions to be assessed separately.

The mRNA will be isolated from samples using the method outlined in Section 2.4 Chapter 1 method. The mRNA samples will be reverse transcribed to cDNA using the High Capacity Reverse Transcription kit (ThermoFisher, Waltham, MA) in 20 μL reactions containing 400 ng of mRNA, according to the manufacturer's instructions. Amplification will be carried out as follows: 10 minutes at 25℃, 120 minutes at 37℃, and then 5 minutes at 85℃.

Quantitative RT-PCR will be performed using Taqman fluorescent hybridization probes (ThermoFisher, Waltham, MA) according to the manufacturer's instructions. The reactions were incubated at 95 ℃ for 10 min followed by 2 min at 50℃. Amplification was then carried out with 50 cycles of 15 seconds at 95℃ and 1 min at 60 ℃. Samples with Ct values higher than 40 cycles will be counted as no expression. Relative mRNA expression will then be calculated using a comparative cycle threshold method (ΔΔCt). All genes and experimental groups will be normalized using 18S as a housekeeping gene. Enteroendocrine cell marker used will be CgA (Chromogranin A), enterochromaffin cells will be denoted with marker 5-HT, and goblet cells will be determined with marker Muc-2.

1.2.4 Scanning Electron Microscopy (SEM) for microvilli

Assessment of microvilli on organoid derived epithelium will be assessed utilizing scanning electron microscopy. Scaffolds will be trimmed in half along lumen then cells will be cross-linked with 2.5% glutaraldehyde. Samples will then be dehydrated for 30 minutes at each of the following ethanol concentrations: 30%, 50%, 75%, 95%, and 2x in 100%. Samples are then to be dried by critical point drying with liquid CO2 dryer (AutoSamdri-815, Tousimis Research Corp.). Samples are then sputter coated with a 10nm thick layer of Pt/Pd (208HR, Cressington Scientific Instruments Inc.). Imaging will be performed using a scanning electron microscope at a voltage of 2~3 kV (Zeiss UltraPlus SEM or Zeiss Supra 55 VP SEM, Carl Zeiss SMT Inc.).

1.3 Preliminary results

Initial co-culture studies were performed in matrigel droplets. Survival of hiNSCs within culture conditions utilized for organoid development would be the most beneficial environment for our studies as the organoid growth and differentiation process is highly sensitive. Immunostaining of general cell markers (TuJ1 for neurons and E-Cad for epithelial cells) within co-culture of hiNSCs and colonoids, indicate compatibility within differentiation medium used to mature the colonoids. Those hiNSCs that were cultured in mono-culture in colonoid differentiation medium, maintain their phenotype with axonal like extensions.

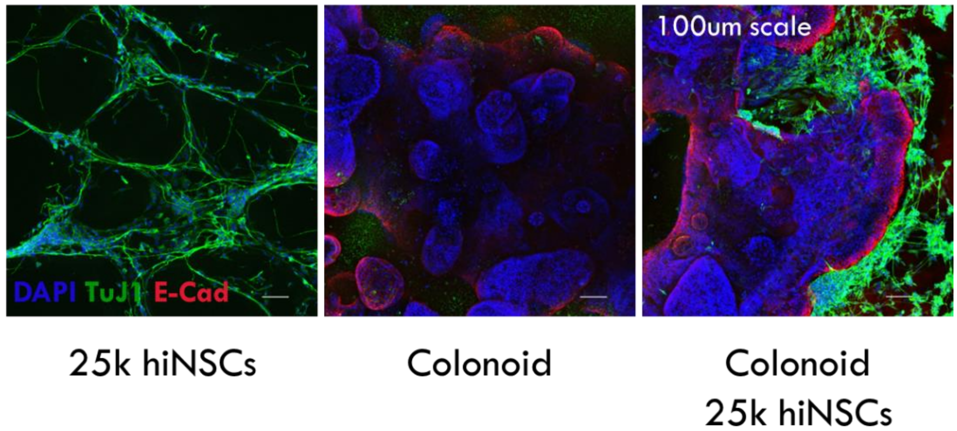

Figure 4-2: Immunostained images of matrigel droplets with or without colonoids, and with or without hiNSC cells are seeded on top. Pan neuronal marker beta III tubulin TUJ1 (green), tight junction marker E-Cad (red) indicates mature epithelium, and nuclear stain DAPI (blue). Scale 100µm.

1.4 Conclusions

Incorporation of an organoid derived epithelial monolayer will allow for further expansion of the populations of cellular interactions we can assess utilizing ivENS scaffolds. Organoids also offer the capabilities to expand cells from patient derived samples to look into the interaction of patient specific epithelium. Past studies have shown that enteric nervous effect the differentiation and development of the epithelium, thus co-culture during the developmental stage of scaffold generation will allow for a more robustly integrated system [9].

The utilization of an epithelium derived organoid would allow for the presence of paneth cells, enterochromaffin cells, and enteroendocrine cells and allows for incorporation of further barrier functions such as mucus production and microvilli polarization. We have not yet explored the various antimicrobial peptides (defensins) that are present within our tissue models, but these epithelial alterations may influence the microbial communities that the ivENS would best support [101]. Defensin secretion is cell type specific, and me be used to elucidate the specific cells that are present within the system via a non-destructive assay. In humans Paneth cells express α-Defensins and mucosal epithelia express β-Defensins [102]. It is unknown as to whether specific enteric neurons express unique defensins.

2 FURTHER CHARACTERIZATION AND NEURAL ACTIVITY

2.1 Background and significance

The full extent of the capabilities of the ivENS systems is not characterized, the addition of spaciotemporal mapping of the cell populations within the scaffolds will expand upon the capabilities that we have been able to showcase thus far. Initial work showcased each test at the various time points originally chosen to show the length with which we could keep the ivENS alive (Calcein AM) and to determine how soon our scaffold maturity was detectable (nNOS at 3 weeks and metabolism at weeks 1, 2, 3). We explored that substance P cascade presence as a potential mechanism that could affect mucus transcription. We did not look into potential epithelial signals that would affect the neuron, but there are potential changes in mucus that might have an effect on neuronal activity as is seen in pulmonary tissue [103]. In order to further characterize the model scaffolds need to be assessed at each week out to 9 weeks for metabolism and scaffolds will be collected at weeks 3, 6, and 9 for Transcriptome Analysis (RNA-Seq). As such we can utilize bioinformatics to assess both factors we have seen in past experiments (nNOS, TuJ1, TAC1, NK1), in addition to some additional markers that indicate maturity such as PGP 9.5 (protein gene product 9.5) and calretinin to further characterize neural maturity [104, 105]. Major neural subtypes arise at different points during development, but the birthdate of some of these neurons is still unknown [105]. By running a transcriptome analysis on our scaffolds, we can run an analysis for known markers now and as the field develops, we can assess new genes of interest from the raw data set. Markers Ki-67 or BrdU (5'-Bromo-2-deoxyuridine) can indicate cell proliferation within the scaffolds that should be increased during development [106]. In addition, we have currently only explored the NK1 receptor transcription -- we can utilize western blot to study the presence of these receptors. If receptors are present, we can use receptor agonists such as Neurokinin A to see if alterations in mucus transcription or mucus thickness are seen in agonist treated conditions [107].

Initially we utilized biomarker TuJ1 to verify that we had a neural population present, but one of the benefits of hiNSCs are that they are a mixed population of cells. As hiNSCs show some glial, neural, and fibroblast populations the effects of these populations on scaffold function is unknown. Glial cells are an important component of the enteric nervous system that can give rise to neurons (*in vivo*) in response to chemical injury that may have links to inflammatory conditions -- we can utilize glial marker brain fatty acid–binding protein (BFABP) or glial fibrillary acidic protein (GFAP) to determine their presence within the system [108]. Should a homogeneous population be required we can remove non-neuronal populations using FACS sorting facilities on the Health Sciences Campus by selecting for the NeuN antibody to separate out neurons prior to seeding [109]. In addition, cultures treated with cytosine arabinoside (Cyt-A) for 4-5 days have been shown to reduce non-neuronal elements by 70%, while allowing neurons with interganglionic fiber strands were to become the main visible constituents in cultures [110]. Both treatment processes remain viable options to limit the amount of non-neuronal cell contaminates.

2.2 Methods

2.2.1 Sample RNA and Protein Extraction

Following culture, in order to isolate RNA and Protein from the ivENS, all samples were rinsed three times with 1x DPBS and flash frozen in microcentrifuge tubes in a liquid nitrogen bath and processed as per Section 2.4 Chapter 1. AllPrep, DNA, RNA, and protein extraction kit (Qiagen, Germantown, MD) will be used to collect the mRNA and Protein following the manufacturer's instructions. Concentration and purity of mRNA will be measured using the ThermoFisher NanoDrop 2000.

2.2.2 Screening via Transcriptome Analysis (RNA-Seq)

The mRNA samples will be sent to the Tufts Genomics Core for Transcriptome Analysis (RNA-Seq). The four conditions studied will include: (a) intestinal cells only, (b) hiNSCs only, (c) co-culture (all listed cell types), and (d) cell free scaffolds.

All scaffolds will be cultured in 1:1 DMEM:SmGM medium, supplemented with 50ng/mL of NGF and 0.2% primocin (Invivogen, San Diego, CA).

2.2.3 Assay of Mucosal Thickness

Samples from the four conditions studied: (a) intestinal cells only, (b) hiNSCs only, (c) co-culture (all listed cell types), and (d) cell free scaffolds, will be assessed using an alcian blue. Samples will be sectioned at 12μm using a Leica CM 1950 cryostat. Embedding will be performed as stated in Section 2.3.2 Chapter 1 using OCT compound (Sakura Finetek). Upon staining sections will be dried for 20 minutes at room temperature followed by a 2 minute rinse in 3% acetic acid. Slides will be stained for 15 minutes in 0.25% Alcian blue 8GX (Sigma-Aldrich, Natick, MA) in 3% acetic acid (ph 2.5). Following staining slides will be removed and dipped in 3% acetic acid then rinsed under running tap water for 10 minutes. Slides will be cover slipped with a DPX mounting medium (Electron Microscopy Sciences, Hatfield, PA) after following a alcohol and xylene series for dehydration and clearing. Measuring the thickness of the mucus on each slice we be done using Alcian blue as described with 3 technical replicates per scaffold and 3 separate biological replicates using light microscopy on a Keyence BZ-X700 microscope [10].

2.2.4 Neural Stimulation

Samples from the four conditions studied: (a) intestinal cells only, (b) hiNSCs only, (c) co-culture (all listed cell types), and (d) cell free scaffolds were grown out to 5 weeks of culture following the protocol outlined in Chapter 1 [47]. For each condition both unstimulated and stimulated protocols were performed at the same time in order to ensure unstimulated samples were subjected to the same environmental conditions as stimulated scaffolds. Recordings were taken over 3 minutes, with chemical and electrical stimulation on treatment scaffolds. All samples with electrical stimulation had the following treatments: baseline recording 1 minute, addition of 50mM potassium gluconate followed by 1 minute of recording, 10Hz stimulation (30 microAmps) for 10 seconds, recording for 1 minute post-stimulation, stop recording. Following recording completion, each sample and the respective unstimulated control were flash frozen in liquid nitrogen for RNA extraction.

Quantitative RT-PCR was performed to quantify the expression of ENS mucosal and substance P (SP) cascade markers in mono-culture and co-culture silk scaffolds. According to Section 2.5 Chapter 2 using Taqman fluorescent hybridization probes (ThermoFisher, Waltham, MA) according to the manufacturer's instructions. The reactions were incubated at 95 ℃ for 10 min followed by 2 min at 50℃. Amplification was then carried out with 50 cycles of 15 seconds at 95℃ and 1 min at 60 ℃. Samples with Ct values higher than 40 cycles were counted as no expression. Relative mRNA expression was then calculated using a comparative cycle threshold method (ΔΔCt). All genes and experimental groups were normalized using 18S as a housekeeping gene. Mucosal marker was Muc-2, and substance P cascade markers include TAC1 and NK-1.

2.3 Preliminary results

Electrical stimulation was performed to stimulate neuronal cells and determine the effect on barrier function and the substance P cascade determined in Chapter 1. We attempted to stimulate the neurons utilizing electrical stimulation and probed changes in following stimulation MUC-2, NK1, and TAC1 via qPCR. Local Field Potential (LFP) was recorded for 3 minutes for each sample with undetectable spikes over baseline noise. Results were inconclusive as the error bars on our samples were too large to determine any statistical significance from the experiments (Figure 4-3, Figure 4-4). NK1 detection was undetermined Ct values ≥ 40.0 for all conditions and analysis could not be performed.

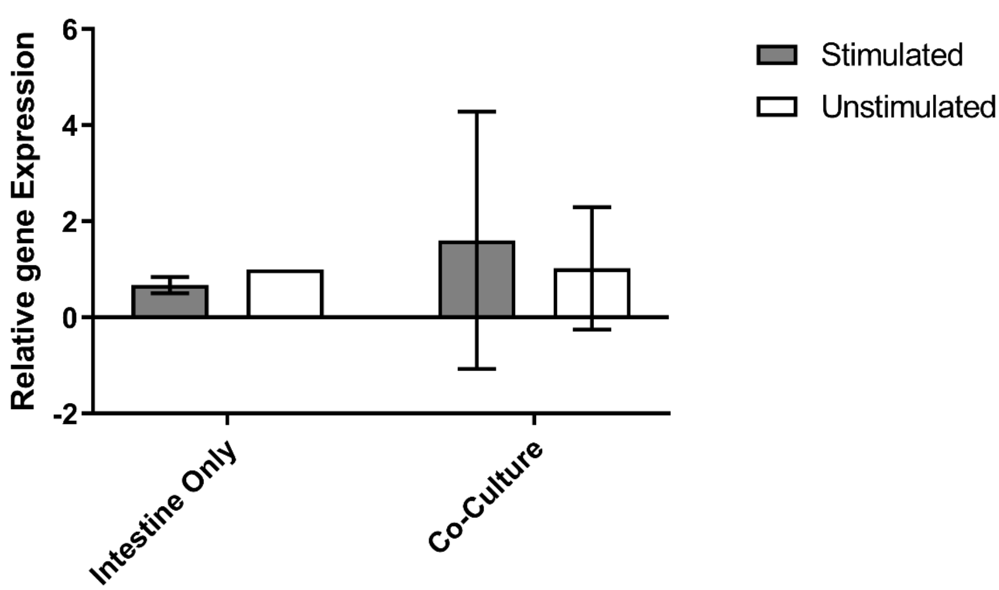

Figure 4-3: Muc2 relative gene expression compared to intestine only unstimulated control. ivENS scaffolds were grown to 5 weeks, samples were

either stimulated or unstimulated, then flash frozen for RNA extraction. Samples were analyzed utilizing 2-way ANOVA, p=0.05, n=3 biological replicates, no significance detected in samples

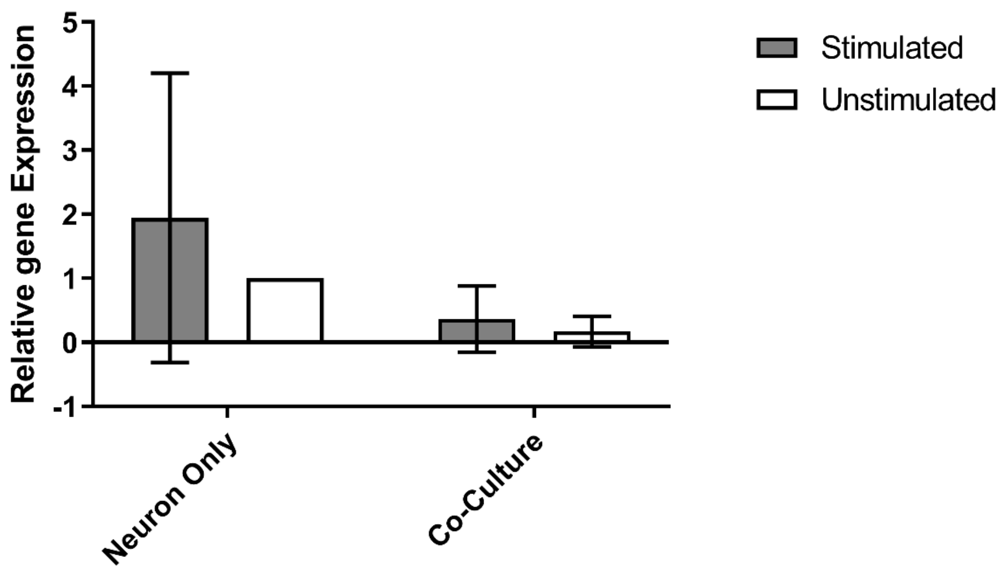

Figure 4-4: Tac1 relative gene expression compared to neuron only unstimulated control. ivENS scaffolds were grown to 5 weeks, samples were either stimulated or unstimulated, then flash frozen for RNA extraction. Samples were analyzed utilizing 2-way ANOVA, p=0.05, n=3 biological replicates for co-culture, n=2 for neuron only, no significance detected in samples.

2.4 Conclusion

Spaciotemporal mapping allows for characterization of the ivENS system that may later be adapted to various projects elucidating the gut-brain axis. Mapping the transcriptome of the course of culture for weeks 3, 6, and 9 will provide a foundation for all future experiments to compare to. By mapping metabolism out to 9 weeks we will determine if the systems may be cultured longer than the previous 60 day mark and have a complete transcriptome signature at various time points during the ivENSs development. With a transcriptome analysis we can determine the ratio with which each gene is expressed at each time point, this will allow us to determine the appropriate timing for experiments the explore the stimulation of neurons.

Past efforts to determine secreted neurotransmitters resulted in concentrations that were too low to confidently detect (**Figure 2-7**). Efforts must be made to not only determine the best time during culture to detect specific cell types, as noted above, but to increase the neural density within the scaffolds. Due to the potential for increased density to emulate disease phenotype or alter the specific sub-populations of enteric neurons present, we need to assess a variety of densities (1 million cells per scaffold is the standard, 2x, 3x, 4x) [40]. In preliminary work we have shown that by increasing the density of our scaffolds, to 2 million cells per scaffold, we are able to detect Fluo-4 Ca2+ response at 5 weeks of culture (video not shown). Fluo-4 experiments can be performed at 2.5 and 5 weeks of culture on the various scaffold densities. In addition, to determine whether the increase in neural density causes pro-inflammatory changes, levels of MCP-1 can be assessed via ELISA.

As we begin to expand upon the system for further studies it is important to maintain appropriate controls as cancer cells have the capability to express some of these markers mentioned (TuJ1, PGP 9.5 and respond to drugs such as tetrodotoxin TTX), intestinal scaffolds free of hiNSCs will be used as a baseline to compare any analysis. Should these intestinal scaffolds express some of the markers used to probe the neural population, we will utilize the intestinal value as a baseline for the scaffolds (3 sections per scaffold, with 3 biological replicates per condition).

Studies that alter the environment or overall oxygen levels, such as hypoxic bioreactor studies, must take into consideration the effect that these treatments will have on cells outside the lumen. We did not assess how depletion of oxygen would affect the neurons within the scaffold. Studies show that capillary networks are less dense between greater vessels on the submucosal level when compared to the myenteric plexus level, but the capillary architecture is heavily associated with the submucosal ganglia that harbor the nNOS neurons [111]. Depletion of oxygen will most likely alter the neural subpopulations that are present, but it might not ablate the neuronal component of the ivENS. Thus, upon addition to the bioreactor this characterization will be done during future work involving low oxygen conditions, as nNOS levels are a subpopulation of particular interest, to run a simple test with and without bioreactor hypoxic flow to determine any change in nNOS presence. The ivENS tissue model is a robust platform, and with the addition of further studies into the exact epithelial and neural architecture present at various timepoints we can cater the system to various needs of studying the enteric nervous system and the gut brain axis.

ACKNOWLEDGMENTS

We would like to thank Dr. Ying Chen, Dr. Dana Cairns, and Terrence Roh with assistance on the colonoid and hiNSC preliminary data. We would also like to thank Dr. Nicolas Rouleau for assistance with the electrical stimulation studies. This work was supported by the NIH (U19AI131126, P41EB002520, R21AI128093, R21AI128342-01, S10 OD021624). We also thank the Gates Foundation for support of these studies. EM was supported by the DoD through the NDSEG Fellowship Program.

CHAPTER 5 APPENDIX OR APPENDICES

1 SEEDING PROTOCOL FOR ivENS SYSTEMS

Intestinal Cell Seeding of ivENS Scaffold

Materials:

1. Confluent human myofibroblasts (Lonza #CC-2902, use between P2-P5)

2. dPBS

3. 0.25% trypsin EDTA (ThermoFisher #25200114)

4. Full DMEM (1x)

5. Collagen-1 solution

6. 10x DMEM medium

7. NaOH (5M)

8. Autoclaved silk intestinal models

9. Autoclaved 2in teflon wires (McMaster #1749T63, cut to 2 or 3 in by machine shop)

10. Petridish

11. Autoclaved tweezers

12. 12-well plate

13. Confluent Caco-2 flask

14. Confluent HT29-MTX flask

15. SmGM (Lonza BulletKit CC-3182 order through Fisher #NC9460389)

16. NGF (stock concentration of 100 µg/mL) (Fisher #256GF100)

17. Primocin (Invivogen #ant-pm-2)

Preparing human intestinal myofibroblasts suspension

1. Remove medium from IMFs
2. Rinse 1x with 10 mL dPBS/T_{175} flask
3. Trypsinize with 5 mL 0.25% trypsin EDTA/T_{175} flask for 3 minutes @ 37℃ with 5% CO_2
4. Quench with 10 mL SmGM medium (can use serum-free DMEM(1X) instead)
5. Count cells (10 µL)

a. (____ + ____ + ____)/3 = ________ x 10^4 cells

b. ________ x 10^4 cells/mL x 15 (volume of trypsin + quenching media) = ________________ cells total

6. Centrifuge IMF cell suspension @ 290 G for 5 minutes
7. Aspirate supernatant
8. Resuspend IMFs in _______ µL of full DMEM(1X) to create a solution of 1 million cells/100 µL as final collagen solution needs to have 1 million cells/mL and the collagen solution is only 10% DMEM(1X) cell suspension

9. Calculate total volume of collagen solution needed ((# of scaffolds + 1) x 300 µL)

10. Calculate volumes of collagen solution components needed:

Total volume: ___________

	Total solution	With cells	Without cells	Total
Collagen	80% total volume			
10X DMEM	10% total volume			
1X DMEM	10% total volume			
NGF (stock concentration of 100 µg/mL)	50ng/mL			

11. Make collagen and DMEM(10x) solution

12. pH solution with 5M NaOH 10 µL at a time

13. Add NGF to solution to create a 50 ng/mL concentration in total collagen solution volume

14. Transfer _______ µL of collagen/DMEM(10x)/NGF solution to a fresh 50 mL conical and label it collagen solution with cells

15. Label original conical collagen solution without cells

16. Add ______ µL of DMEM(1x) to cell-free conical

17. Add ______ µL of IMF cell suspension in DMEM(1x) to conical labeled collagen solution with cells

Human IMF seeding

1. Place appropriate number of scaffolds on petri dishes labeled w/cells or w/o cells
2. Plug the lumen of the sterilized silk intestinal models with sterile teflon wires
3. Suction out the DI water in scaffolds, using flat side of tweezers to press down on scaffold as water is suctioned out
4. Saturate each cell-free scaffold with 300 µL of cell-free collagen solution
5. Saturate each w/cell scaffold with 300 µL of IMF cell suspension collagen solution
6. Incubate scaffolds @ 37℃ with 5% CO_2 for 30 minutes to get collagen solution to gel

Preparing epithelial cell suspension

1. Aspirate medium from both caco-2 and HT29-MTX flasks
2. Rinse 1x with 10 mL dPBS/T_{175} flask
3. Trypsinize with 5 mL 0.25% trypsin EDTA/T_{175} flask for 10 minutes @ 37℃ with 5% CO_2
4. Quench each separately with 10 mL/T_{175} of full DMEM (1x)

5. Count cells (10 µL) for each cell type

Caco-2

a. (____ + ____ + ____) / 3 = ________ x 10^4 cells

b. ________ x 10^4 cells / mL x 15 (volume of trypsin + quenching media) = ________________ cells total

HT29-MTX

c. (____ + ____ + ____) / 3 = ________ x 10^4 cells

d. ________ x 10^4 cells / mL x 15 (volume of trypsin + quenching media) = ________________ cells total

4. Centrifuge each cell suspension @ 290 G for 5 minutes

5. Calculate total volume of epithelial cell solution needed ((# of cell scaffolds + 1) x 200 µL), can also add more volume here to make sure you will have enough

6. Determine # of cells per mL by dividing total # of cells by mL of solution they are suspended in

7. Determine # of cells needed in final solution volume to have 1.5 million Caco-2 cells/mL and 0.5 million HT29-MTX cells/mL and then calculate the volume of final cell suspension needed to get this many cells

8. Make final epithelial cell suspension solution with 3:1 Caco-2:HT29-MTX by adding appropriate amounts of cell suspensions and then filling the rest of the volume with full DMEM(1x)

Epithelial layer seeding

1. Take the scaffolds out of the incubator and place back in hood
2. Pipette 100 µL of epithelial cells suspension into the lumen of all w/cell scaffolds, try to avoid spilling the solution outside the lumen or creating bubbles in the lumen
3. Pipette 100 µL of DMEM (1x) into the lumen of all w/o cell scaffolds, try to avoid spilling the solution outside the lumen or creating bubbles in the lumen
4. Pipette out any excess pools of cell suspension below the scaffolds
5. Incubate scaffolds @ 37℃ with 5% CO_2 for one hour
6. Take scaffolds out of incubator and place back in hood
7. Flip all scaffolds 180 degrees
8. Pipette 100 µL of epithelial cells suspension into the lumen of all w/cell scaffolds, try to avoid spilling the solution outside the lumen or creating bubbles in the lumen

9. Pipette 100 µL of DMEM (1x) into the lumen of all w/o cell scaffolds, try to avoid spilling the solution outside the lumen or creating bubbles in the lumen
10. Pipette out any excess pools of cell suspension below the scaffolds
11. Incubate scaffolds @ 37℃ with 5% CO_2 for one hour

Intestinal model feeding

1. Take scaffolds out of incubator and place back in hood
2. Using tweezers, place each scaffold in appropriately labeled well of 12-well plate with lumen parallel to ground
3. Make 1:1 SmGM:DMEM(1x) solution with 0.2% primocin and 50 ng/mL of NGF (stock concentration of 100 µg/mL)
4. Pipette 3 mL of 1:1 SmGM:DMEM(1x) solution into each well
5. Incubate scaffolds @ 37℃ with 5% CO_2
6. Feed scaffolds with 1:1 SmGM:DMEM(1x) solution every other day

hiNSC Seeding of ivENS Scaffold

The hiNSC seeding within the scaffolds is performed 7 days following intestinal cell seeding.

Materials

1. Full DMEM (1x)

2. dPBS

3. TrypLE (1x) (Gibco #12563-011)

4. Collagen-1 solution

5. 10X DMEM medium

6. NaOH (5M)

7. SmGM (Lonza BulletKit CC-3182 order through Fisher #NC9460389)

8. Petridish

9. Autoclaved tweezers

10. 12-well plate

11. NGF (stock concentration of 100 µg/mL) (Fisher #256GF100)

12. Primocin (Invivogen #ant-pm-2)

Preparing hiNSC cell suspension

1. Aspirate old medium

2. 10 mL dPBS rinse

3. 6 mL trypsin LE (1x) : 1 min @ 37℃ with 5% CO_2

4. Scrape with serological pipette while in trypsin

5. Quench with 12 mL serum-free DMEM

6. Spin down @ 25℃ @1200 rpm for 5 minutes (can spin again if pellet does not form)

7. Count cells (10 µL)

a. (____ + ____ + ____) / 3 = ________ x 10^4 cells

b. ________ x 10^4 cells / mL x 18 (volume of trypsin + quenching media) = ________________ cells total - make collagen for this.

c. When preparing cells for collagen all cells are added to 1x DMEM so that 1 million cells/10uL will be 1 millions cell/100 uL in final collagen solution

8. Calculate volume of collagen solution needed for hiNSC seeding (add 20% for pipette error):

. 80% collagen = ______ µL

a. 10% 10x DMEM = ______ µL

b. 10% 1x DMEM = ______ µL

9. Calculate volumes of collagen solution needed for blank seeding (add 20% for pipette error):

. 80% collagen = ______ µL

a. 10% 10x DMEM = ______ µL

b. 10% 1x DMEM = ______ µL

10. Make the collagen and 10x DMEM solution and pH with 5M NaOH (10 uL at a time). Keep collagen solutions on ice throughout seeding
11. Using the calculations above, split collagen solution into one conical for adding hiNSC cell suspension and one conical for adding blank DMEM
12. Add the 10% DMEM with hiNSC cell suspension to appropriate conical of collagen solution
13. Add the 10% DMEM cell-free solution to appropriate conical of collagen solution

hiNSC seeding

1. Remove scaffolds from medium and place in petri dishes, separating the cell-free and
2. Add 25 uL of collagen solution with hiNSC cell suspension to top side of appropriate scaffolds
3. Add 25 uL of blank collagen solution to top side of appropriate scaffolds
4. Incubate all scaffolds for 10 minutes @ 37℃ with 5% CO_2
5. Take scaffolds out of incubator and rotate scaffolds 90 degrees.
6. Repeat steps 3-5 until all four sides of scaffolds have been seeded.
7. Add 3 mL/well$_{12}$ of 1:1 SmGM:DMEM + 50 ng/mL NGF + 0.2% primocin
8. Incubate overnight @ 37℃ with 5% CO_2

CHAPTER 6 BIBLIOGRAPHY

BIBLIOGRAPHY

[1] H. Wang, I.-S. Lee, C. Braun, P. Enck, Effect of Probiotics on Central Nervous System Functions in Animals and Humans: A Systematic Review, J Neurogastroenterol Motil 22(4) (2016) 589-605.
[2] J. Khlevner, Y. Park, K.G. Margolis, Brain-Gut Axis: Clinical Implications, Gastroenterology clinics of North America 47(4) (2018) 727-739.
[3] E.A. Mayer, K. Tillisch, A. Gupta, Gut/brain axis and the microbiota, The Journal of clinical investigation 125(3) (2015) 926-38.
[4] T.H.M.P. Consortium, Structure, function and diversity of the healthy human microbiome, Nature 486(7402) (2012) 207-14.
[5] N. Sudo, Y. Chida, Y. Aiba, J. Sonoda, N. Oyama, X.-N. Yu, C. Kubo, Y. Koga, Postnatal microbial colonization programs the hypothalamic-pituitary-adrenal system for stress response in mice, The Journal of physiology 558(Pt 1) (2004) 263-275.
[6] M. Carabotti, A. Scirocco, M.A. Maselli, C. Severi, The gut-brain axis: interactions between enteric microbiota, central and enteric nervous systems, Ann Gastroenterol 28(2) (2015) 203-209.
[7] N.J. Yang, I.M. Chiu, Bacterial Signaling to the Nervous System through Toxins and Metabolites, Journal of molecular biology 429(5) (2017) 587-605.
[8] M.J. Workman, M.M. Mahe, S. Trisno, H.M. Poling, C.L. Watson, N. Sundaram, C.-F. Chang, J. Schiesser, P. Aubert, E.G. Stanley, A.G. Elefanty, Y. Miyaoka, M.A. Mandegar, B.R. Conklin, M. Neunlist, S.A. Brugmann, M.A. Helmrath, J.M. Wells, Engineered human pluripotent-stem-cell-derived intestinal tissues with a functional enteric nervous system, Nature Medicine 23(1) (2017) 49-59.
[9] M. Puzan, S. Hosic, C. Ghio, A. Koppes, Enteric Nervous System Regulation of Intestinal Stem Cell Differentiation and Epithelial Monolayer Function, Sci Rep 8(1) (2018) 6313.
[10] Y. Chen, Y. Lin, K.M. Davis, Q. Wang, J. Rnjak-Kovacina, C. Li, R.R. Isberg, C.A. Kumamoto, J. Mecsas, D.L. Kaplan, Robust bioengineered 3D functional human intestinal epithelium, Scientific Reports 5 (2015) 13708.
[11] M.A. DeCicco RePass, Y. Chen, Y. Lin, W. Zhou, D.L. Kaplan, H.D. Ward, Novel Bioengineered Three-Dimensional Human Intestinal Model for Long-Term Infection of Cryptosporidium parvum, Infection and immunity 85(3) (2017).
[12] L. Shaban, Y. Chen, A.C. Fasciano, Y. Lin, D.L. Kaplan, C.A. Kumamoto, J. Mecsas, A 3D intestinal tissue model supports Clostridioides difficile germination, colonization, toxin production and epithelial damage, Anaerobe 50 (2018) 85-92.
[13] E. Manousiouthakis, D.L. Kaplan, Engineering the Gut-Brain Axis, In Preparation (2019).
[14] E.A. Mayer, Gut feelings: the emerging biology of gut–brain communication, Nature Reviews Neuroscience 12(8) (2011) 453-66.

[15] A.J. Burns, A.M. Goldstein, D.F. Newgreen, L. Stamp, K.-H. Schafer, M. Metzger, R. Hotta, H.M. Young, P.W. Andrews, N. Thapar, J. Belkind-Gerson, N. Bondurand, J.C. Bornstein, W.Y. Chan, K. Cheah, M.D. Gershon, R.O. Heuckeroth, R.M.W. Hofstra, L. Just, R.P. Kapur, S.K. King, C.J. McCann, N. Nagy, E. Ngan, F. Obermayr, V. Pachnis, P.J. Pasricha, M.H. Sham, P. Tam, P. Vanden Berghe, White paper on guidelines concerning enteric nervous system stem cell therapy for enteric neuropathies, Developmental biology 417(2) (2016) 229-51.
[16] W. El-Nachef, T. Grikscheit, Enteric nervous system cell replacement therapy for Hirschsprung disease: beyond tissue-engineered intestine, European journal of pediatric surgery : official journal of Austrian Association of Pediatric Surgery ... [et al] = Zeitschrift fur Kinderchirurgie 24(3) (2014) 214-8.
[17] S.R. Merker, J. Weitz, D.E. Stange, Gastrointestinal organoids: How they gut it out, Developmental biology 420(2) (2016) 239-250.
[18] S. Gonkowski, Substance P as a neuronal factor in the enteric nervous system of the porcine descending colon in physiological conditions and during selected pathogenic processes, BioFactors (Oxford, England) 39(5) (2013) 542-51.
[19] H. Han, C. Pan, C. Liu, X. Lv, X. Yang, Y. Xiong, Y. Lu, W. Wu, J. Han, Z. Zhou, H. Jiang, L. Zhang, Y. Zhao, Gut-neuron interaction via Hh signaling regulates intestinal progenitor cell differentiation in Drosophila, Cell discovery 1 (2015) 15006.
[20] E. Zakhem, S. Raghavan, K.N. Bitar, Neo-innervation of a bioengineered intestinal smooth muscle construct around chitosan scaffold, Biomaterials 35(6) (2014) 1882-9.
[21] E. Zakhem, M. Elbahrawy, G. Orlando, K.N. Bitar, Successful implantation of an engineered tubular neuromuscular tissue composed of human cells and chitosan scaffold, Surgery 158(6) (2015) 1598-608.
[22] N. Yissachar, Y. Zhou, L. Ung, N.Y. Lai, J.F. Mohan, A. Ehrlicher, D.A. Weitz, D.L. Kasper, I.M. Chiu, D. Mathis, C. Benoist, An Intestinal Organ Culture System Uncovers a Role for the Nervous System in Microbe-Immune Crosstalk, Cell 168(6) (2017) 1135-1148.e12.
[23] D.M. Cairns, K. Chwalek, Y.E. Moore, M.R. Kelley, R.D. Abbott, S. Moss, D.L. Kaplan, Expandable and rapidly differentiating human induced neural stem cell lines for multiple tissue engineering applications, Stem Cell Reports 7(3) (2016) 557-570.
[24] D.N. Rockwood, R.C. Preda, T. Yucel, X. Wang, M.L. Lovett, D.L. Kaplan, Materials fabrication from Bombyx mori silk fibroin, Nature protocols 6(10) (2011) 1612-31.
[25] F.G. Omenetto, D.L. Kaplan, New opportunities for an ancient material, Science (New York, N.Y.) 329(5991) (2010) 528-31.
[26] M.D. Tang-Schomer, J.D. White, L.W. Tien, L.I. Schmitt, T.M. Valentin, D.J. Graziano, A.M. Hopkins, F.G. Omenetto, P.G. Haydon, D.L. Kaplan, Bioengineered functional brain-like cortical tissue, Proceedings of the National Academy of Sciences of the United States of America 111(38) (2014) 13811-6.

[27] V.E. Bosio, J. Brown, M.J. Rodriguez, D.L. Kaplan, Biodegradable Porous Silk Microtubes for Tissue Vascularization, Journal of materials chemistry. B 5(6) (2017) 1227-1235.
[28] M. McGill, N. Raol, K.S. Gipson, S.N. Bowe, J. Fulk-Logan, A. Nourmahnad, J.Y. Chung, M.J. Whalen, D.L. Kaplan, C.J. Hartnick, Preclinical assessment of resorbable silk splints for the treatment of pediatric tracheomalacia, The Laryngoscope (2018).
[29] W. Siran, C.E. Ghezzi, D.M. Cairns, R.E. Pollard, Y. Chen, R. Gomes, T.B. McKay, D. Pouli, A. Jamali, I. Georgakoudi, J.L. Funderburgh, K. Kenyon, P. Hamrah, D.L. Kaplan, Human Corneal Tissue Model for Nociceptive Assessments, Advanced healthcare materials 7(19) (2018) e1800488.
[30] N.R. Raia, B.P. Partlow, M. McGill, E.P. Kimmerling, C.E. Ghezzi, D.L. Kaplan, Enzymatically crosslinked silk-hyaluronic acid hydrogels, Biomaterials 131 (2017) 58-67.
[31] S.E.L. Vidal, K.A. Tamamoto, H. Nguyen, R.D. Abbott, D.M. Cairns, D.L. Kaplan, 3D biomaterial matrix to support long term, full thickness, immuno-competent human skin equivalents with nervous system components, Biomaterials 198 (2019) 194-203.
[32] K. Chwalek, M.D. Tang-Schomer, F.G. Omenetto, D.L. Kaplan, In vitro bioengineered model of cortical brain tissue, Nature protocols 10(9) (2015) 1362-73.
[33] W.L. Cantley, C. Du, S. Lomoio, T. DePalma, E. Peirent, D. Kleinknecht, M. Hunter, M.D. Tang-Schomer, G. Tesco, D.L. Kaplan, Functional and Sustainable 3D Human Neural Network Models from Pluripotent Stem Cells, ACS Biomaterials Science & Engineering 4(12) (2018) 4278-4288.
[34] M.D. Gershon, The enteric nervous system: a second brain, Hospital practice (1995) 34(7) (1999) 31-2, 35-8, 41-2 passim.
[35] M. Rao, M.D. Gershon, Enteric nervous system development: what could possibly go wrong?, Nat Rev Neurosci 19(9) (2018) 552-565.
[36] S. Pompolo, J.B. Furness, Ultrastructure and synaptic relationships of calbindin-reactive, Dogiel type II neurons, in myenteric ganglia of guinea-pig small intestine, J Neurocytol 17(6) (1988) 771-82.
[37] Z.S. Li, C. Schmauss, A. Cuenca, E. Ratcliffe, M.D. Gershon, Physiological modulation of intestinal motility by enteric dopaminergic neurons and the D2 receptor: analysis of dopamine receptor expression, location, development, and function in wild-type and knock-out mice, J Neurosci 26(10) (2006) 2798-807.
[38] C. Mongardi Fantaguzzi, M. Thacker, R. Chiocchetti, J.B. Furness, Identification of neuron types in the submucosal ganglia of the mouse ileum, Cell and tissue research 336(2) (2009) 179-89.
[39] E.A. Accili, N. Dhatt, A.M. Buchan, Neural somatostatin, vasoactive intestinal polypeptide and substance P in canine and human jejunum, Neuroscience letters 185(1) (1995) 37-40.
[40] K.G. Margolis, K. Stevanovic, N. Karamooz, Z.S. Li, A. Ahuja, F. D'Autreaux, V. Saurman, A. Chalazonitis, M.D. Gershon, Enteric neuronal density contributes to

the severity of intestinal inflammation, Gastroenterology 141(2) (2011) 588-98, 598.e1-2.
[41] F.R. Demehri, I.F. Halaweish, A.G. Coran, D.H. Teitelbaum, Hirschsprung-associated enterocolitis: pathogenesis, treatment and prevention, Pediatric surgery international 29(9) (2013) 873-81.
[42] S.E. Lakhan, A. Kirchgessner, Neuroinflammation in inflammatory bowel disease, Journal of neuroinflammation 7 (2010) 37.
[43] K. Geboes, S. Collins, Structural abnormalities of the nervous system in Crohn's disease and ulcerative colitis, Neurogastroenterology and Motility 10(3) (1998) 189-202.
[44] H.P. Browne, S.C. Forster, B.O. Anonye, N. Kumar, B.A. Neville, M.D. Stares, D. Goulding, T.D. Lawley, Culturing of 'unculturable' human microbiota reveals novel taxa and extensive sporulation, Nature 533(7604) (2016) 543-546.
[45] C.A. Lozupone, J.I. Stombaugh, J.I. Gordon, J.K. Jansson, R. Knight, Diversity, stability and resilience of the human gut microbiota, Nature 489(7415) (2012) 220-30.
[46] P. Louis, G.L. Hold, H.J. Flint, The gut microbiota, bacterial metabolites and colorectal cancer, Nature reviews. Microbiology 12(10) (2014) 661-72.
[47] E. Manousiouthakis, Y. Chen, D. Cairns, R. Pollard, K. Gerlovin, M. Dente, Y. Razavi, D.L. Kaplan, Bioengineered In Vitro Enteric Nervous System, Journal of Tissue Engineering and Regenerative Medicine (2019).
[48] A.M. Urbanska, F. Sefat, S. Yousaf, S. Kargozar, P.B. Milan, M. Mozafari, Nanoengineered biomaterials for intestine regeneration, in: M. Mozafari, J. Rajadas, D. Kaplan (Eds.), Nanoengineered Biomaterials for Regenerative Medicine, Elsevier2019, pp. 363-378.
[49] M.M. Hao, H.M. Young, Development of enteric neuron diversity, Journal of Cellular and Molecular Medicine. 13(7) (2009) 1193-210.
[50] M. Anlauf, M.K. Schafer, L. Eiden, E. Weihe, Chemical coding of the human gastrointestinal nervous system: cholinergic, VIPergic, and catecholaminergic phenotypes, The Journal of comparative neurology 459(1) (2003) 90-111.
[51] J.P. Timmermans, J. Hens, D. Adriaensen, Outer submucous plexus: an intrinsic nerve network involved in both secretory and motility processes in the intestine of large mammals and humans, The Anatomical record 262(1) (2001) 71-8.
[52] J.B. Furness, G.J. Sanger, Intrinsic nerve circuits of the gastrointestinal tract: identification of drug targets, Current opinion in pharmacology 2(6) (2002) 612-22.
[53] S.J. Brookes, Classes of enteric nerve cells in the guinea-pig small intestine, The Anatomical record 262(1) (2001) 58-70.
[54] F. Martel, R. Monteiro, C. Lemos, Uptake of Serotonin at the Apical and Basolateral Membranes of Human Intestinal Epithelial (Caco-2) Cells Occurs through the Neuronal Serotonin Transporter (SERT), Journal of Pharmacology and Experimental Therapeutics 306(1) (2003) 355-362.

[55] P. Habibovic, H. Yuan, C.M. van der Valk, G. Meijer, C.A. van Blitterswijk, K. de Groot, 3D microenvironment as essential element for osteoinduction by biomaterials, Biomaterials 26(17) (2005) 3565-3575.
[56] S. Bartfeld, H. Clevers, Stem cell-derived organoids and their application for medical research and patient treatment, Journal of molecular medicine (Berlin, Germany) 95(7) (2017) 729-738.
[57] M.A. Lancaster, J.A. Knoblich, Organogenesis in a dish: modeling development and disease using organoid technologies, Science (New York, N.Y.) 345(6194) (2014) 1247125.
[58] A.L. Man, E. Bertelli, S. Rentini, M. Regoli, G. Briars, M. Marini, A.J. Watson, C. Nicoletti, Age-associated modifications of intestinal permeability and innate immunity in human small intestine, Clinical science (London, England : 1979) 129(7) (2015) 515-27.
[59] S. Jangi, R. Gandhi, L.M. Cox, N. Li, F. von Glehn, R. Yan, B. Patel, M.A. Mazzola, S. Liu, B.L. Glanz, S. Cook, S. Tankou, F. Stuart, K. Melo, P. Nejad, K. Smith, B.D. Topcuolu, J. Holden, P. Kivisakk, T. Chitnis, P.L. De Jager, F.J. Quintana, G.K. Gerber, L. Bry, H.L. Weiner, Alterations of the human gut microbiome in multiple sclerosis, Nature communications 7 (2016) 12015.
[60] T.G. Dinan, J.F. Cryan, Gut instincts: microbiota as a key regulator of brain development, ageing and neurodegeneration, The Journal of physiology 595(2) (2017) 489-503.
[61] M.C. Houser, M.G. Tansey, The gut-brain axis: is intestinal inflammation a silent driver of Parkinson's disease pathogenesis?, NPJ Parkinson's disease 3 (2017) 3.
[62] N. Lahar, N.Y. Lei, J. Wang, Z. Jabaji, S.C. Tung, V. Joshi, M. Lewis, M. Stelzner, M.G. Martin, J.C. Dunn, Intestinal subepithelial myofibroblasts support in vitro and in vivo growth of human small intestinal epithelium, PloS one 6(11) (2011) e26898.
[63] C.A. Cobine, G.W. Hennig, M. Kurahashi, K.M. Sanders, S.M. Ward, K.D. Keef, Relationship between interstitial cells of Cajal, fibroblast-like cells and inhibitory motor nerves in the internal anal sphincter, Cell and tissue research 344(1) (2011) 17-30.
[64] K.A. Sharkey, P.L. Beck, D.M. McKay, Neuroimmunophysiology of the gut: advances and emerging concepts focusing on the epithelium, Nature reviews. Gastroenterology & hepatology 15(12) (2018) 765-784.
[65] Y. Chen, W. Zhou, T. Roh, M.K. Estes, D.L. Kaplan, In vitro enteroid-derived three-dimensional tissue model of human small intestinal epithelium with innate immune responses, PloS one 12(11) (2017) e0187880.
[66] G.J. Mahler, M.L. Shuler, R.P. Glahn, Characterization of Caco-2 and HT29-MTX cocultures in an in vitro digestion/cell culture model used to predict iron bioavailability, The Journal of nutritional biochemistry 20(7) (2009) 494-502.
[67] R. Soret, S. Coquenlorge, F. Cossais, G. Meurette, M. Rolli-Derkinderen, M. Neunlist, Characterization of human, mouse, and rat cultures of enteric glial cells and their effect on intestinal epithelial cells, Neurogastroenterology and motility

: the official journal of the European Gastrointestinal Motility Society 25(11) (2013) e755-64.
[68] M.W. Mulholland, G. Romanchuk, K. Lally, D.M. Simeone, Nerve growth factor promotes neurite outgrowth in guinea pig myenteric plexus ganglia, The American journal of physiology 267(4 Pt 1) (1994) G716-22.
[69] T.A. Heanue, I.T. Shepherd, A.J. Burns, Enteric nervous system development in avian and zebrafish models, Developmental biology 417(2) (2016) 129-38.
[70] A.S. Wallace, A.J. Burns, Development of the enteric nervous system, smooth muscle and interstitial cells of Cajal in the human gastrointestinal tract, Cell and tissue research 319(3) (2005) 367-82.
[71] P.S. Kabouridis, V. Pachnis, Emerging roles of gut microbiota and the immune system in the development of the enteric nervous system, The Journal of clinical investigation 125(3) (2015) 956-64.
[72] Y. Ou, R. Liu, N. Wei, X. Li, O. Qiang, W. Huang, C. Tang, Effects of octreotide on nitric oxide synthase expression in the small intestine of high fat diet-induced obese rats, Obesity research & clinical practice 6(4) (2012) e263-346.
[73] P. Plaisancie, J. Claustre, M. Estienne, G. Henry, R. Boutrou, A. Paquet, J. Leonil, A novel bioactive peptide from yoghurts modulates expression of the gel-forming MUC2 mucin as well as population of goblet cells and Paneth cells along the small intestine, The Journal of nutritional biochemistry 24(1) (2013) 213-21.
[74] P. Holzer, U. Holzer-Petsche, Tachykinins in the gut. Part I. Expression, release and motor function, Pharmacology & therapeutics 73(3) (1997) 173-217.
[75] E. Goldin, F. Karmeli, Z. Selinger, D. Rachmilewitz, Colonic substance P levels are increased in ulcerative colitis and decreased in chronic severe constipation, Digestive diseases and sciences 34(5) (1989) 754-7.
[76] A. Kawabata, M. Kinoshita, H. Nishikawa, R. Kuroda, M. Nishida, H. Araki, N. Arizono, Y. Oda, K. Kakehi, The protease-activated receptor-2 agonist induces gastric mucus secretion and mucosal cytoprotection, The Journal of clinical investigation 107(11) (2001) 1443-50.
[77] M. Davoodian, N. Boroumand, M. Mehrabi Bahar, A.H. Jafarian, M. Asadi, S.I. Hashemy, Evaluation of serum level of substance P and tissue distribution of NK-1 receptor in breast cancer, Molecular biology reports 46(1) (2019) 1285-1293.
[78] E. Manousiouthakis, N. Alden, M. Dente, O. Hofheinz, R. Menon, E. Callaway, C. Cheng, A. Jayaraman, K. Lee, D.L. Kaplan, Effect of microbial metabolites on in vitro enteric nervous system tissue model, In Preparation (2019).
[79] A.K. Nash, T.A. Auchtung, M.C. Wong, D.P. Smith, J.R. Gesell, M.C. Ross, C.J. Stewart, G.A. Metcalf, D.M. Muzny, R.A. Gibbs, N.J. Ajami, J.F. Petrosino, The gut mycobiome of the Human Microbiome Project healthy cohort, Microbiome 5(1) (2017) 153.
[80] R.M. Jones, The Influence of the Gut Microbiota on Host Physiology: In Pursuit of Mechanisms, The Yale journal of biology and medicine 89(3) (2016) 285-297.

[81] K.M. Neufeld, N. Kang, J. Bienenstock, J.A. Foster, Reduced anxiety-like behavior and central neurochemical change in germ-free mice, Neurogastroenterology and motility : the official journal of the European Gastrointestinal Motility Society 23(3) (2011) 255-64, e119.
[82] W.H. Liu, H.L. Chuang, Y.T. Huang, C.C. Wu, G.T. Chou, S. Wang, Y.C. Tsai, Alteration of behavior and monoamine levels attributable to Lactobacillus plantarum PS128 in germ-free mice, Behavioural brain research 298(Pt B) (2016) 202-9.
[83] A.J. Brown, S.M. Goldsworthy, A.A. Barnes, M.M. Eilert, L. Tcheang, D. Daniels, A.I. Muir, M.J. Wigglesworth, I. Kinghorn, N.J. Fraser, N.B. Pike, J.C. Strum, K.M. Steplewski, P.R. Murdock, J.C. Holder, F.H. Marshall, P.G. Szekeres, S. Wilson, D.M. Ignar, S.M. Foord, A. Wise, S.J. Dowell, The Orphan G protein-coupled receptors GPR41 and GPR43 are activated by propionate and other short chain carboxylic acids, The Journal of biological chemistry 278(13) (2003) 11312-9.
[84] E. d'Hennezel, S. Abubucker, L.O. Murphy, T.W. Cullen, Total Lipopolysaccharide from the Human Gut Microbiome Silences Toll-Like Receptor Signaling, mSystems 2(6) (2017).
[85] T.A. Faraj, C. Stover, C. Erridge, Dietary Toll-Like Receptor Stimulants Promote Hepatic Inflammation and Impair Reverse Cholesterol Transport in Mice via Macrophage-Dependent Interleukin-1 Production, Frontiers in immunology 10 (2019) 1404.
[86] P.J. Kennedy, J.F. Cryan, T.G. Dinan, G. Clarke, Kynurenine pathway metabolism and the microbiota-gut-brain axis, Neuropharmacology 112(Pt B) (2017) 399-412.
[87] P.V. Chang, L. Hao, S. Offermanns, R. Medzhitov, The microbial metabolite butyrate regulates intestinal macrophage function via histone deacetylase inhibition, Proceedings of the National Academy of Sciences of the United States of America 111(6) (2014) 2247-52.
[88] N. Alden, S. Krishnan, V. Porokhin, R. Raju, K. McElearney, A. Gilbert, K. Lee, Biologically Consistent Annotation of Metabolomics Data, Analytical chemistry 89(24) (2017) 13097-13104.
[89] M. Levy, E. Blacher, E. Elinav, Microbiome, metabolites and host immunity, Current opinion in microbiology 35 (2017) 8-15.
[90] G.A. Cresci, E. Bawden, Gut Microbiome: What We Do and Don't Know, Nutrition in clinical practice : official publication of the American Society for Parenteral and Enteral Nutrition 30(6) (2015) 734-46.
[91] J.F. Burgueno, A. Barba, E. Eyre, C. Romero, M. Neunlist, E. Fernandez, TLR2 and TLR9 modulate enteric nervous system inflammatory responses to lipopolysaccharide, Journal of neuroinflammation 13(1) (2016) 187.
[92] M. Stephens, P.Y. von der Weid, Lipopolysaccharides modulate intestinal epithelial permeability and inflammation in a species-specific manner, Gut microbes (2019) 1-12.
[93] P. Brun, S. Gobbo, V. Caputi, L. Spagnol, G. Schirato, M. Pasqualin, E. Levorato, G. Palu, M.C. Giron, I. Castagliuolo, Toll like receptor-2 regulates

production of glial-derived neurotrophic factors in murine intestinal smooth muscle cells, Molecular and cellular neurosciences 68 (2015) 24-35.
[94] H. Roume, A. Heintz-Buschart, E.E. Muller, P. Wilmes, Sequential isolation of metabolites, RNA, DNA, and proteins from the same unique sample, Methods in enzymology 531 (2013) 219-36.
[95] J.B. Furness, Types of neurons in the enteric nervous system, Journal of the autonomic nervous system 81(1-3) (2000) 87-96.
[96] T. Sato, R.G. Vries, H.J. Snippert, M. van de Wetering, N. Barker, D.E. Stange, J.H. van Es, A. Abo, P. Kujala, P.J. Peters, H. Clevers, Single Lgr5 stem cells build crypt-villus structures in vitro without a mesenchymal niche, Nature 459(7244) (2009) 262-5.
[97] T. Tsuruta, S. Saito, Y. Osaki, A. Hamada, A. Aoki-Yoshida, K. Sonoyama, Organoids as an ex vivo model for studying the serotonin system in the murine small intestine and colon epithelium, Biochemical and biophysical research communications 474(1) (2016) 161-167.
[98] E. Fiorica-Howells, R. Hen, J. Gingrich, Z. Li, M.D. Gershon, 5-HT(2A) receptors: location and functional analysis in intestines of wild-type and 5-HT(2A) knockout mice, Am J Physiol Gastrointest Liver Physiol 282(5) (2002) G877-93.
[99] S.H. Rhee, C. Pothoulakis, E.A. Mayer, Principles and clinical implications of the brain-gut-enteric microbiota axis, Nature reviews. Gastroenterology & hepatology 6(5) (2009) 306-14.
[100] S. Schneider, C.M. Wright, R.O. Heuckeroth, Unexpected Roles for the Second Brain: Enteric Nervous System as Master Regulator of Bowel Function, Annu Rev Physiol 81 (2019) 235-259.
[101] I.S. Larsen, A.M. Fritzen, C.S. Carl, M. Agerholm, M.T.F. Damgaard, J.B. Holm, A. Marette, P. Nordkild, B. Kiens, K. Kristiansen, J. Wehkamp, B.A.H. Jensen, Human Paneth cell alpha-defensin-5 treatment reverses dyslipidemia and improves glucoregulatory capacity in diet-induced obese mice, Am J Physiol Endocrinol Metab 317(1) (2019) E42-e52.
[102] N.H. Salzman, M.A. Underwood, C.L. Bevins, Paneth cells, defensins, and the commensal microbiota: a hypothesis on intimate interplay at the intestinal mucosa, Semin Immunol 19(2) (2007) 70-83.
[103] J. Barrios, K.R. Patel, L. Aven, R. Achey, M.S. Minns, Y. Lee, V.E. Trinkaus-Randall, X. Ai, Early life allergen-induced mucus overproduction requires augmented neural stimulation of pulmonary neuroendocrine cell secretion, Faseb j 31(9) (2017) 4117-4128.
[104] P. Vento, S. Soinila, Quantitative comparison of growth-associated protein GAP-43, neuron-specific enolase, and protein gene product 9.5 as neuronal markers in mature human intestine, J Histochem Cytochem 47(11) (1999) 1405-16.
[105] A.J. Bergner, L.A. Stamp, D.G. Gonsalvez, M.B. Allison, D.P. Olson, M.G. Myers, Jr., C.R. Anderson, H.M. Young, Birthdating of myenteric neuron subtypes in the small intestine of the mouse, The Journal of comparative neurology 522(3) (2014) 514-27.

[106] N. Kee, S. Sivalingam, R. Boonstra, J.M. Wojtowicz, The utility of Ki-67 and BrdU as proliferative markers of adult neurogenesis, J Neurosci Methods 115(1) (2002) 97-105.
[107] N.M.J. Rupniak, E. Perdona, C. Griffante, P. Cavallini, A. Sava, D.J. Ricca, K.B. Thor, E.C. Burgard, M. Corsi, Affinity, potency, efficacy, and selectivity of neurokinin A analogs at human recombinant NK2 and NK1 receptors, PloS one 13(10) (2018) e0205894.
[108] C. Laranjeira, K. Sandgren, N. Kessaris, W. Richardson, A. Potocnik, P. Vanden Berghe, V. Pachnis, Glial cells in the mouse enteric nervous system can undergo neurogenesis in response to injury, The Journal of clinical investigation 121(9) (2011) 3412-24.
[109] D. Guez-Barber, S. Fanous, B.K. Harvey, Y. Zhang, E. Lehrmann, K.G. Becker, M.R. Picciotto, B.T. Hope, FACS purification of immunolabeled cell types from adult rat brain, J Neurosci Methods 203(1) (2012) 10-8.
[110] F.L. Christofi, M. Hanani, N. Maudlej, J.D. Wood, Enteric glial cells are major contributors to formation of cyclic AMP in myenteric plexus cultures from adult guinea-pig small intestine, Neuroscience letters 159(1-2) (1993) 107-10.
[111] S. Jabari, W. Neuhuber, A. Brehmer, Neurovascular Interface in Porcine Small Intestine: Specific for Nitrergic rather than Nonnitrergic Neurons, Cells Tissues Organs 201(3) (2016) 203-10.